

Effect of Erythropoietin on Cisplatin Induced Nephrotoxicity in Adult Male Albino Rat: Histological, Ultrastructural and Biochemical Study

Original
Article

Hossam Yahia Sayed Emam

Department of Anatomy, Faculty of Medicine, Cairo University, Egypt.

ABSTRACT

Introduction: Cisplatin is documented as an effective chemotherapeutic drug with many adverse effects on vital organs, including nephrotoxicity, neurotoxicity and ototoxicity. Erythropoietin is a glycoprotein hormone synthesized by the renal fibroblasts in the interstitial tissue of the renal cortex in response to hypoxia. Recent research work points out that it could to improve the renal dysfunction and histopathological alterations caused by oxidative stress.

Aim: Is to examine the possible protective role of erythropoietin in cases with cisplatin induced nephrotoxicity.

Materials and Methods: The present study used fifty adult male albino rats, with their weights within the range of 180-220 g. The rats were divided into five groups, 10 rats each: Group I (Control group): Each of the rats in this group received a single intraperitoneal injection of a normal saline solution (0.9% sodium chloride). Group II (Cisplatin administration group): Each of the rats in this group was injected once with cisplatin intraperitoneally at a dose of 6 mg/kg. Group III (Cisplatin and erythropoietin pre-administration group): Rats of this group were injected with a single dose of erythropoietin; 3000 IU/kg intraperitoneally, and one day later they were injected with 6 mg/kg of cisplatin intraperitoneally. Group IV (Cisplatin and erythropoietin co-administration group): Rats of this group were injected with a single dose of erythropoietin; 3000 IU/kg intraperitoneally together with 6 mg/kg of cisplatin by the same rout. Group V (Erythropoietin and cisplatin post-administration group): Rats of this group were injected with a single dose of 3000 IU/kg erythropoietin intraperitoneally, and five days later they were given 6 mg/kg of cisplatin by the same rout.

Results: Cisplatin injection exerted various histopathological and laboratory alterations such as renal tubular cell necrosis, nuclear pyknosis and cytoplasmic vacuolation as well as marked elevation of levels of blood urea and serum creatinine. Erythropoietin could improve all the histopathological and functional deterioration exerted by cisplatin injection especially when given prior to cisplatin administration.

Conclusion: Erythropoietin could prevent the adverse histological and functional alterations induced by intraperitoneal injection of cisplatin in the kidney of adult male albino rat.

Key Words: Cisplatin, erythropoietin, kidney.

Revised: 1 September 2019, **Accepted:** 3 December 2019.

Corresponding Author: Hossam Yahia Sayed Emam, MD, Department of Anatomy, Faculty of Medicine, Cairo University, Egypt, **Tel.:** 00201223621228, **E-mail:** hossam.yahia@kasralainy.edu.eg

ISSN: 2536-9172, June 2021, Vol. 5, No. 1

INTRODUCTION

Cisplatin is documented as an effective chemotherapeutic agent for neoplasms arising from different tissues. However treatment with cisplatin is well documented to cause many adverse effects in vital organs, mainly nephrotoxicity, neurotoxicity and ototoxicity. Cisplatin-induced nephrotoxicity is the most prevalent adverse effect, where more than 30% of patients treated with it have been reported to develop acute kidney injury after the administration of this drug. Treatment with cisplatin is reported to induce renal tubular cell damage, which is more pronounced in the cells of the proximal convoluted tubules than in the cells of the other renal tubules. Moreover, it exerts marked elevation of blood levels of creatinine and urea several days after its administration. Several in vivo and in vitro research studies elucidated that

oxidative stress is the most important factor contributing to cisplatin-induced renal tubular cell damage. Reported mechanisms by which cisplatin exerts its deleterious effect are the activation of oxidative enzymes (e.g. NADPH oxidase enzyme) as well as increasing the generation of reactive oxygen species (ROS), which both subject cellular macromolecules (mainly lipids and proteins) to oxidative stress that could be severe enough to induce cell death (Hanigan and Devarajan, 2003; Mishima *et al.*, 2006; Pabla and Dong, 2008; Rashed *et al.*, 2011; Cao *et al.*, 2018 and Sonoda *et al.*, 2019). Erythropoietin is a glycoprotein hormone synthesized by fibroblasts in the interstitial tissue of the renal cortex in response to hypoxia. Recombinant human erythropoietin (rhEPO) has been used as a successful therapy in end-stage renal failure and cancer chemotherapy with or without association with anaemia. Clinical research studies proved that rhEPO can

improve the renal dysfunction and histological alterations emanating from oxidative stress. Moreover, it could ameliorate the pathological changes exerted by various nephrotoxic drugs and in case of diabetic nephropathy and progressive glomerulonephritis (Rjiba-Touati *et al*, 2011; De Nicola and Zoccali, 2016; Vecchio and Zuccala, 2017).

MATERIALS AND METHODS

Chemicals:

1- Cisplatin: was obtained as a vial of 10mg/10ml solution (Unistin; EIMC United Pharmaceuticals, Badr city, Cairo, ARE). It was given in a single intraperitoneal dose of 6mg/ kg (Rjiba-Touati *et al*, 2011)

2- Erythropoietin: was available as recombinant human erythropoietin vials (10.000 IU/ml), provided by the Egyptian Pharmex Company, imported from Shenyang Sunshine Pharmaceutical Co., China. It was given as a single dose of 3000 IU/ kg intaperitoneally (Rjiba-Touati *et al*, 2011).

Animals:

The current study used fifty adult male albino rats, with their weights within the range of 180-220 g. They were obtained from the animal house, Faculty of Medicine, Cairo University. The rats were housed in separate cages and were kept under standard laboratory and environmental conditions with standard rat chow. The rats were divided into five groups 10 rats each:

Group I (Control group): Rats of this group received nothing more than water and food.

Group II (Cisplatin administration group): Rats of this group received single injection of 6 mg/kg cisplatin intaperitoneally.

Group III (Cisplatin and erythropoietin pre-administration group): Rats of this group received a single dose of 3000 IU/ kg erythropoietin intaperitoneally, followed the day after by an injection of 6 mg/kg of cisplatin intaperitoneally.

Group IV (Cisplatin and erythropoietin co-administration group): Rats of this group were injected with a single dose of 3000 IU/ kg erythropoietin intaperitoneally, given simultaneously with of 6 mg/kg of cisplatin given by the same rout.

Group V (Erythropoietin and cisplatin post-administration group): Rats of this group were injected with a single dose of 3000 IU/ kg erythropoietin intaperitoneally, and five days later they were given a dose of 6 mg/kg of cisplatin by the same rout.

At the last day of the experiment, the rats were sacrificed by cervical dislocation, and the kidneys were removed and processed for light, electron microscopic and histomorphometric studies. Rats of groups I, II and IV were sacrificed at day five, rats of groups III were sacrificed at day six, while those of group V were sacrificed at day ten.

Methods:

The kidneys were excised and processed for the following studies:

1- Light microscopic study; using haematoxylin and eosin as well as toluidine blue stains

2- Electron microscopic examination; specimens from both kidneys were obtained then cut into small slices that were fixed in 4% glutaraldehyde solution, then washed in phosphate buffer and post-fixed in 1% osmium tetroxide. After fixation, specimens were dehydrated and embedded in epoxy resins. Semithin sections of 1 µm thickness were stained with toluidine blue. Finally, ultrathin sections of 60 nm thickness were prepared and stained with uranyl acetate and lead citrate (Winning *et al*, 2016). The sections were examined and photographed using a Joel, 100 CX II transmission.

3- Biochemical study; blood samples were collected from the dorsal pedal veins of the rats into tubes for assessment of blood levels of urea and creatinine

Statistical analysis:

The collected data was organized, tabulated and statistically analyzed with SPSS software statistical computer package version 22 (SPSS Inc, USA). The mean and standard deviation were calculated. ANOVA (Analysis of variance) was used to test the difference about mean values of measured parameters among groups, multiple comparison between pairs of groups were performed using Tukey HSD (Post hoc range test). For interpretation of results of tests of significance, significance was adopted at $P \leq 0.05$.

RESULTS

1- Results of histological and ultrastructural studies:

Group I (Control group): Light microscopic examination of the renal cortex stained with haematoxylin & eosin and semithin sections stained with toluidine blue displayed renal corpuscles formed of dense rounded glomeruli surrounded by Bowman's capsules with average urinary spaces in-between. Proximal convoluted tubules were lined by cuboidal cells with strongly acidophilic cytoplasm and spherical basal nuclei. The distal convoluted tubules were lined with low cuboidal cells with

faint acidophilic cytoplasm and rounded central nuclei. Intact apical brush borders were detected in the proximal convoluted tubules in semithin sections (**Figs. 1 and 2**). Electron microscopic examination of proximal convoluted tubular cells displayed rounded heterochromatic nuclei with prominent nucleoli and intact nuclear envelopes, abundant parallel mitochondria and intact basal infoldings. Apical intact microvilli were observed in the cells of the proximal convoluted tubules (**Fig. 3**).

Light microscopic examination of the renal medulla stained with haematoxylin & eosin and semithin sections presented collecting tubules lined with simple columnar epithelium, and loops of Henle lined with simple cuboidal epithelium with scanty cytoplasm (**Figs 4 and 5**). Electron microscopic examination of an epithelial lining cell of the ascending limb of loop of Henle displayed heterochromatic nuclei with prominent nucleoli and intact nuclear envelopes. The cytoplasm showed abundant mitochondria within normal appearance (**Fig. 6**).

Group II (Cisplatin administration group): Light microscopic examination of the renal cortex stained with haematoxylin & eosin and semithin sections displayed extremely shrunken glomeruli with widened urinary spaces. Most of proximal and distal convoluted tubules are markedly dilated, and their cells exhibited pyknotic nuclei and extensive cytoplasmic vacuolation. Proximal convoluted tubules showed loss of the apical brush border, with epithelial cell exfoliation into tubular lumen. Interstitial tissue exudates were detected (**Figs. 7 and 8**). Electron microscopic examination of proximal convoluted tubular cells displayed shrunken nuclei with indented nuclear membranes. The cytoplasm showed extensive cytoplasmic rarefaction with marked decrease of mitochondria, with the remaining mitochondria appeared ballooned with damaged cristae. The basolateral membrane was thick irregular, while the apical membrane showed marked loss of apical microvilli (**Fig. 9**). Light microscopic examination of the renal medulla stained with haematoxylin & eosin and semithin sections presented loops of Henle and collecting tubules with intra-luminal casts, completely degenerated lining epithelial cells, nuclear pyknosis and exfoliated cells into the lumen. Interstitial tissue showed marked infiltration by fibroblasts and mononuclear cells (**Figs. 10 and 11**). Electron microscopic examination of an epithelial lining cell of the ascending limb of loop of Henle displayed markedly degenerated nuclei, extensive cytoplasmic rarefaction, markedly ballooned mitochondria with complete loss of cristae and markedly thick irregular basal cell membrane (**Fig. 12**).

Group III (Cisplatin and erythropoietin pre-administration group): Light microscopic examination of the renal cortex stained with haematoxylin & eosin and semithin sections presented apparently normal renal

corpuscles with rounded glomeruli and apparently normal urinary spaces. Proximal and distal convoluted tubules exhibited a near normal appearance with intact apical brush borders in the proximal tubules. Few epithelial cells exhibited cytoplasmic vacuolation, pyknotic nuclei and exfoliation into the tubular lumen (**Figs. 13 and 14**). Electron microscopic examination of proximal convoluted tubular cells displayed intact apical microvilli, mild cytoplasmic rarefaction, apparently normal heterochromatic nuclei with prominent nucleoli and intact regular nuclear envelopes. Most of the mitochondria appeared normal while few appeared ballooned with destroyed cristae. A uniformly thin basal cell membrane and intact basal infoldings were observed (**Figs. 15 and 16**). Light microscopic examination of the renal medulla stained with haematoxylin & eosin and semithin sections presented apparently normal loops of Henle and collecting tubules. Few of them exhibited intraluminal casts and exfoliation into the lumen of renal tubules (**Figs. 17 and 18**). Electron microscopic examination of an epithelial lining cell of the ascending limb of loop of Henle displayed heterochromatic nucleus with intact nuclear envelope, mild cytoplasmic rarefaction, and abundant mitochondria with intact cristae (**Fig. 19**).

Group IV (Cisplatin and erythropoietin co-administration group): Light microscopic examination of the renal cortex stained with haematoxylin & eosin and semithin sections displayed moderately shrunken and congested glomeruli surrounded by a mildly dilated urinary space. Some of proximal and distal convoluted tubules were dilated, while others were collapsed and showed intraluminal casts and exfoliated epithelial cells. Some of the lining cells showed pyknotic nuclei and cytoplasmic vacuolation, while others appeared normal with intact apical brush borders. Extravasated blood was detected in-between the renal tubules (**Figs. 20 and 21**). Electron microscopic examination of proximal convoluted tubular cells displayed heterochromatic nuclei with prominent nucleoli and intact nuclear envelopes, partially damaged apical microvilli and marked cytoplasmic rarefaction. Some mitochondria appeared normal with intact cristae while others were ballooned with damaged cristae (**Fig. 22**). Light microscopic examination of the renal medulla stained with haematoxylin & eosin and semithin sections presented collapsed and degenerated renal tubules with intra-luminal casts and exfoliated cells into their lumina. Some of the cells appeared normal while others displayed pyknotic nuclei (**Figs. 23 and 24**). Electron microscopic examination of an epithelial lining cell of the ascending limb of loop of Henle displayed nuclei with peripherally clumped chromatin and intact nuclear envelope, apparently normal mitochondria and moderate cytoplasmic rarefaction. Intact basal infoldings and a uniform thin basal cell membrane were observed (**Fig. 25**).

Group V (Cisplatin and erythropoietin post-administration group): Light microscopic examination

of the renal cortex stained with haematoxylin & eosin and semithin sections presented shrunken glomeruli surrounded by a widened urinary space. Most of proximal and distal convoluted tubules exhibited intraluminal casts and exfoliated cells with cytoplasmic vacuolation. Some of renal corpuscles, proximal and distal convoluted tubules were apparently normal. The proximal tubules exhibited intact apical brush borders in most of the cells. Interstitial tissue exudates were detected (Figs. 26 and 27). Electron microscopic examination of proximal convoluted tubular cells displayed karyolytic nuclei with disrupted nuclear envelopes, marked cytoplasmic rarefaction and apparently normal mitochondria with few of them swollen with destroyed cristae (Fig. 28). Light microscopic examination of the renal medulla stained with haematoxylin & eosin and semithin sections presented few apparently normal loops of Henle and collecting tubules, while most of them appeared collapsed and degenerated with intraluminal casts. Congested blood vessels inbetween tubules were observed (Figs. 29 and 30). Electron microscopic examination of an epithelial lining cell of the ascending limb of loop of Henle displayed a nucleus having clumped chromatin and disrupted nuclear envelope, thick irregular basal cell membrane. Some mitochondria were apparently normal while others were ballooned with lost cristae (Fig. 31).

2) Results of the biochemical study

Blood urea was statistically significantly higher in group II (97.38 ± 10.93), IV (45.72 ± 5.67) and group

V (56.62 ± 20.51) compared to group I (18.48 ± 2.65), $p < 0.0001$, 0.008 and < 0.0001 , respectively. There was no statistically significant difference between the group I and group III ($p = 0.806$). On the other hand, Blood urea was statistically significantly lower in group III (26.24 ± 6.7), group IV (45.72 ± 5.67) and group V (56.62 ± 20.51) compared to group II (97.38 ± 10.93), $p < 0.0001$. Blood urea was statistically significantly higher in group V (2.32 ± 0.32) compared to group III (4.78 ± 0.46), $p = 0.003$. But there was no statistically significant difference between the group III and group IV ($p = 0.080$). Also, there was no statistically significant difference between the group IV and group V ($p = 0.546$) (Figs. 32, 33).

Serum creatinine was statistically significantly higher in group II (3.6 ± 0.77), group IV (3.02 ± 0.78) and group V (2.83 ± 0.52) compared to group I (0.57 ± 0.1), $p < 0.0001$. There was no statistically significant difference between the group I and group III ($p = 0.976$). Serum creatinine was statistically significantly lower in group III (0.78 ± 0.12) compared to group II (3.6 ± 0.77), $p < 0.0001$. However there was no statistically significant difference between the group II with group IV and group V ($p = 0.467$ and 207 , respectively). Serum creatinine also was statistically significantly higher in group IV (3.02 ± 0.78) and group V (2.83 ± 0.52) compared to group III (0.78 ± 0.12), $p < 0.0001$. There was no statistically significant difference between the group IV and group V ($p = 0.980$) (Figs. 34 and 35).

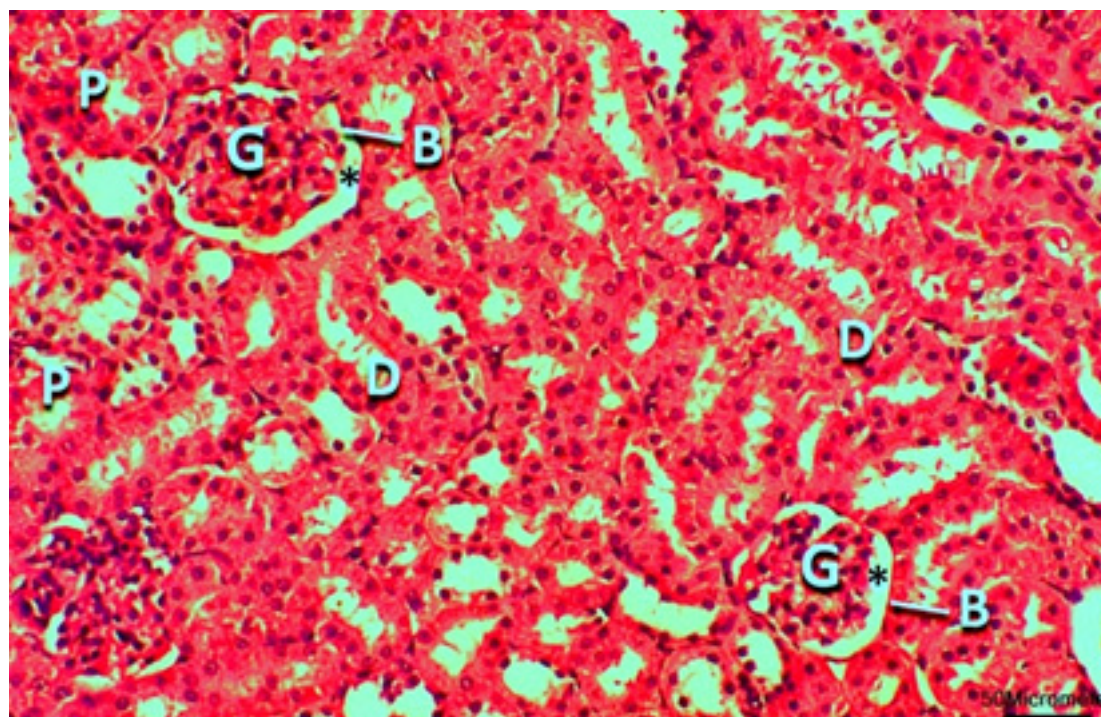


Fig. 1: A photomicrograph of a cross section of the renal cortex of a rat of group I (Control group) showing renal corpuscles, formed of a dense rounded glomerulus (G) surrounded by a parietal layer of Bowman's capsule (B) with the urinary Bowman's space in-between (*). Proximal convoluted tubules (P) are lined with cuboidal cells with strongly acidophilic cytoplasm and spherical basal nuclei. The distal convoluted tubules (D) are lined with low cuboidal cells with acidophilic cytoplasm and rounded central nuclei (Hx.&E. X200)

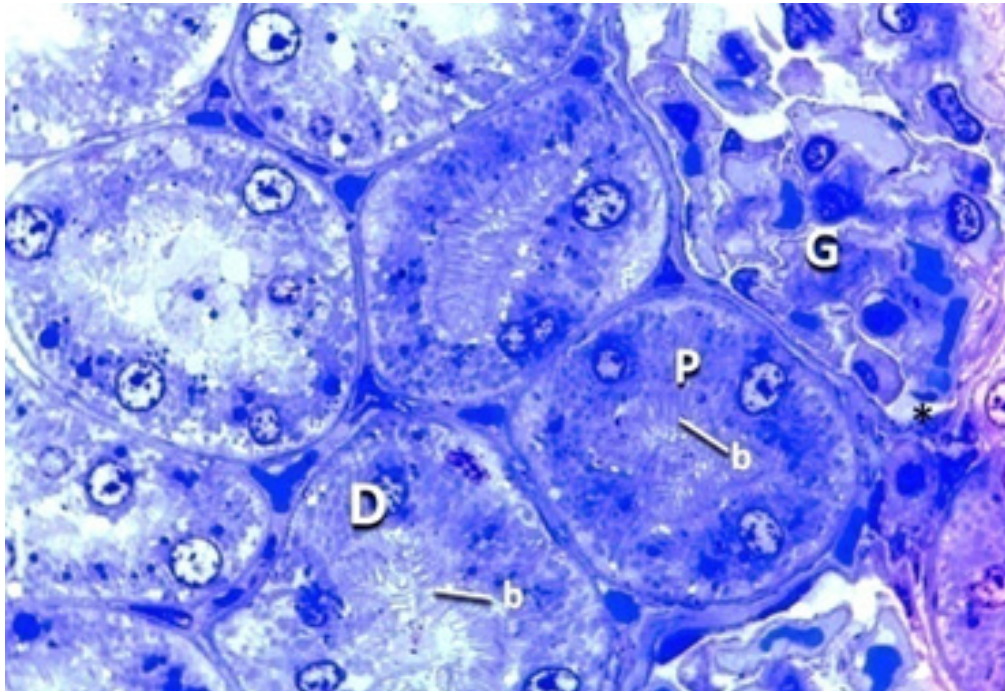


Fig. 2: A photomicrograph of a semithin section of the renal cortex of a rat of group I demonstrating part of a glomerulus (G) of a renal corpuscle. The proximal convoluted tubules (P) are deeply stained and display an intact apical brush border (b), while distal convoluted tubules are faintly stained and lack a brush border (Toluidine blue X1000).

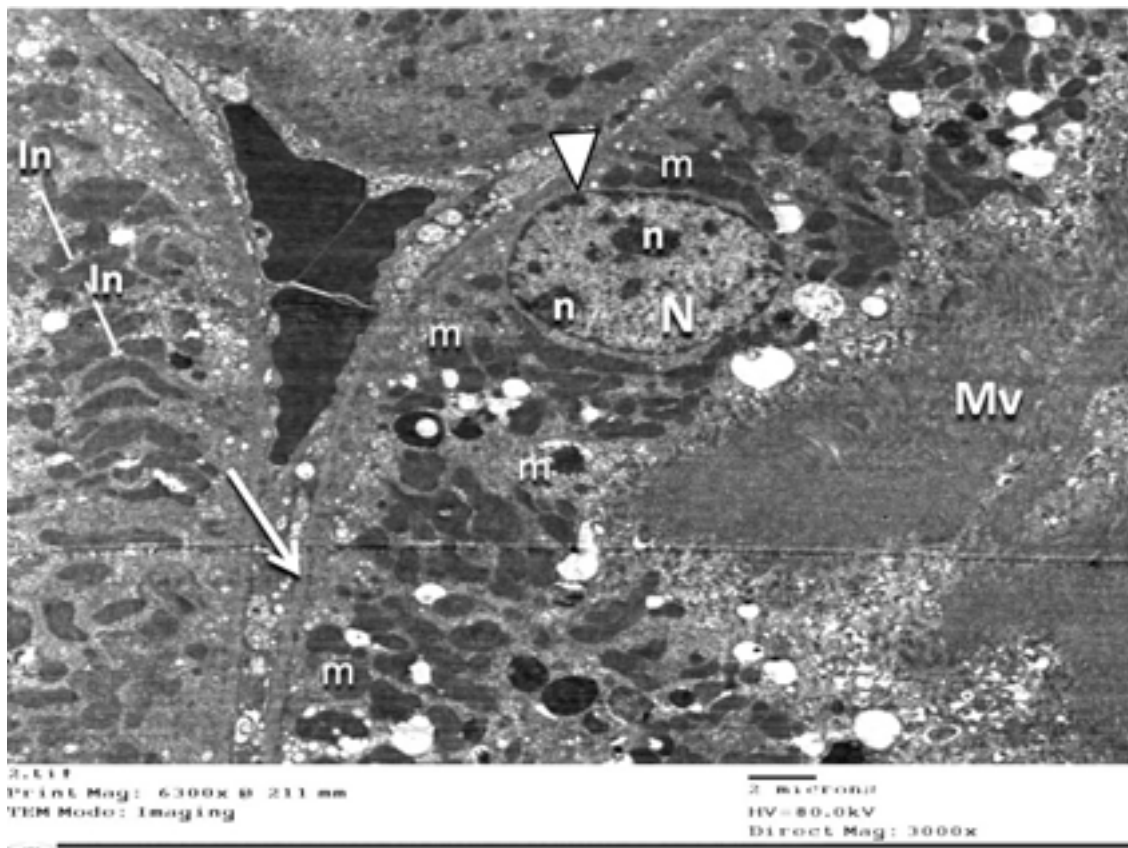


Fig. 3: An electron micrograph of a rat kidney of group I displaying a proximal convoluted tubular cell with rounded heterochromatic nucleus (N) with prominent nucleolus (n) and intact nuclear envelop (arrowhead), abundant parallel electron dense mitochondria (m), and a uniformly thin basal cell membrane (thin arrow). Intact basal infoldings (In) and intact apical microvilli (Mv) can be seen (EM X 3000).

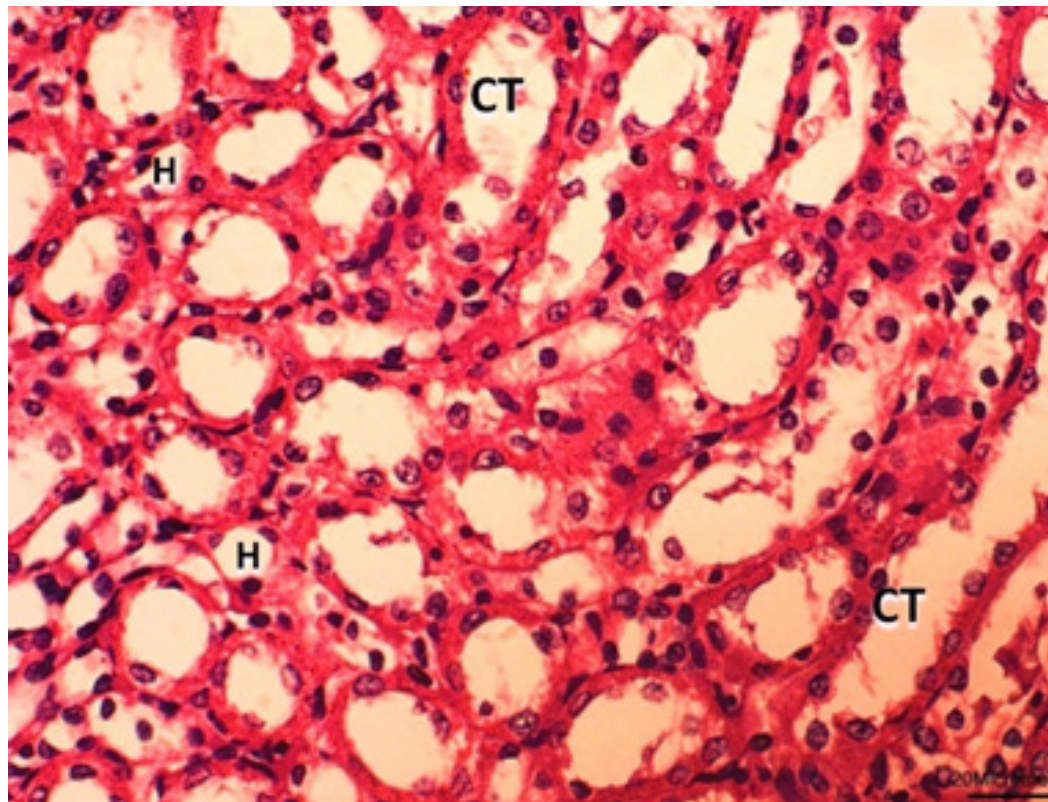


Fig. 4: A photomicrograph of a cross section of the renal medulla of a rat of group I featuring collecting tubules (CT) lined with simple low columnar epithelium and loops of Henle (H) lined with simple cuboidal epithelium with scanty cytoplasm (Hx.&E. X400).

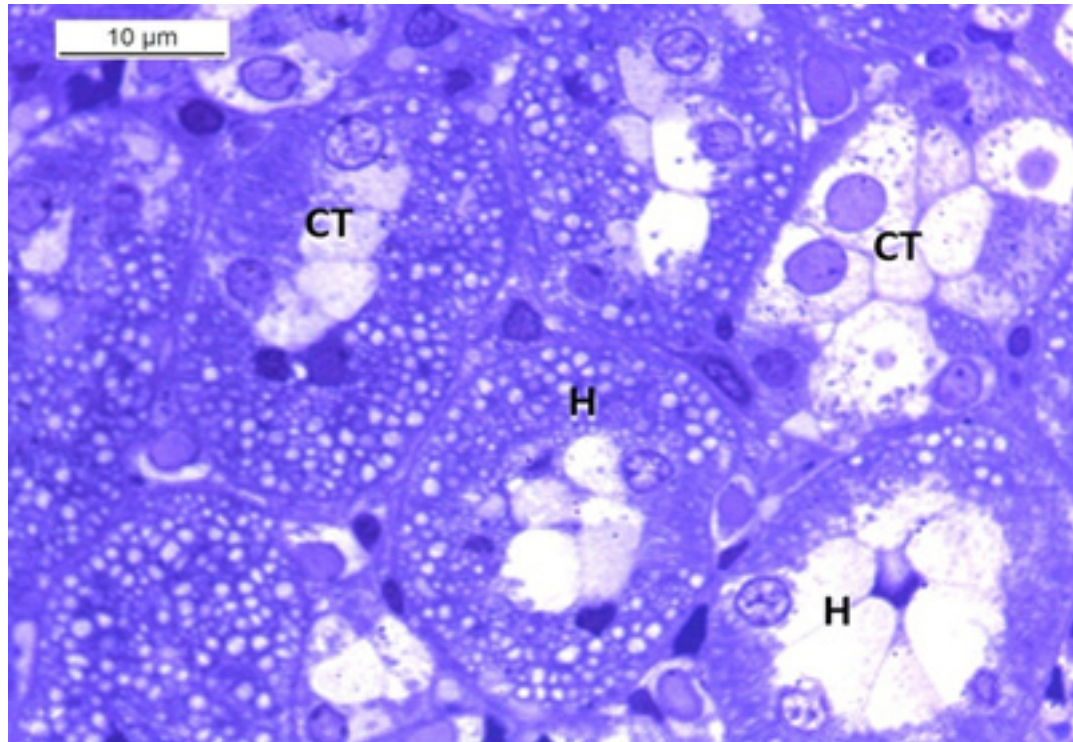


Fig. 5: A photomicrograph of a semithin section of the renal medulla of group I showing collecting tubules (CT) lined with low columnar epithelium and loops of Henle (H) lined with low columnar epithelium (Toluidine blue x 1000).

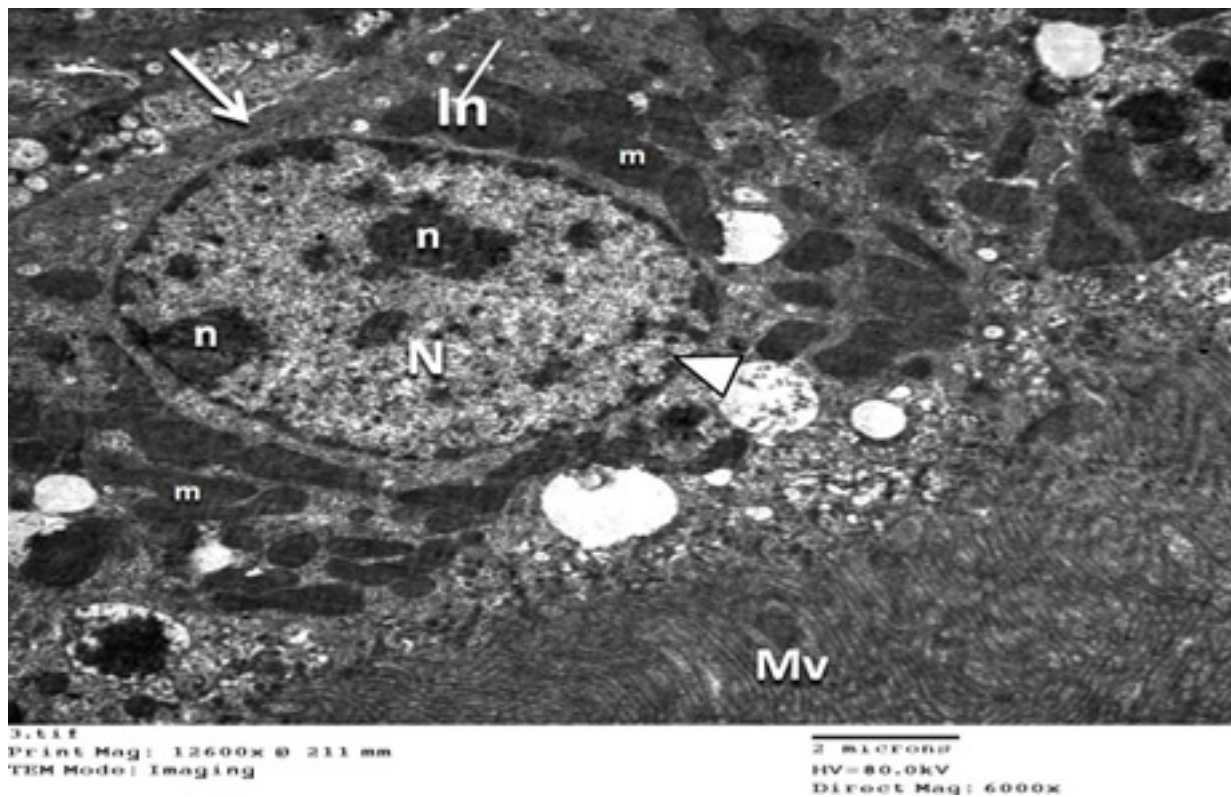


Fig. 6: An electron micrograph of the renal medulla of a rat of group I displaying an epithelial lining cell of the ascending limb of loop of Henle with a heterochromatic nucleus (N) showing prominent nucleoli (n) and intact nuclear envelop (arrowhead). Basal infoldings (In) and few apical microvilli (Mv) can be seen. The basal cell membrane is clear and uniform (thin arrow). The cytoplasm contains abundant electron dense mitochondria (m) with intact cristae (EM X6000).

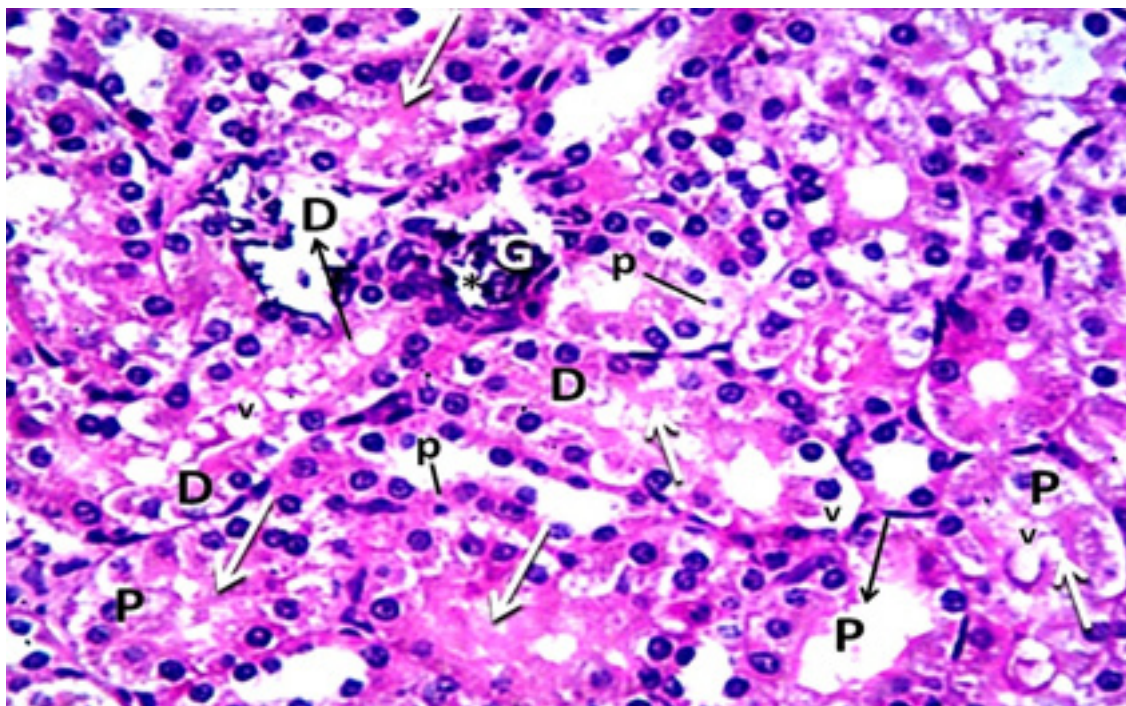


Fig. 7: A photomicrograph of a cross section of the renal cortex of a rat of group II (Cisplatin administration group) showing extremely shrunken glomeruli (G) with a widened urinary space (*). Most of the proximal (P) and distal (D) convoluted tubules are markedly dilated (black arrows) with pyknotic nuclei (p) and cytoplasmic vacuolations (v). The brush border is disrupted in most of the proximal tubules (Hx.&E. X 400)

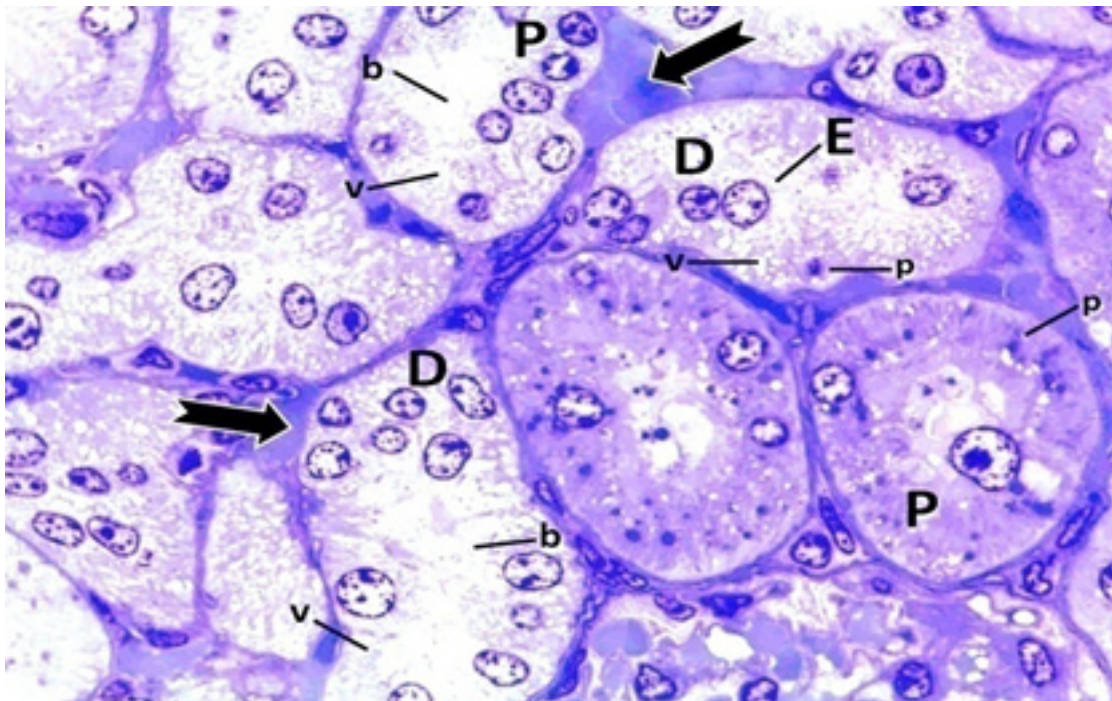


Fig. 8: A photomicrograph of a semithin section of the renal cortex of a rat of group II demonstrating proximal (P) and distal (D) convoluted tubules, with loss of the apical brush border (b) from the proximal tubules. Cells of the tubules show nuclear pyknosis (p), extensive cytoplasmic vacuolation (V) and epithelial cell exfoliation into tubular lumen (E). The thick notched arrows indicate interstitial tissue exudates (Toluidine blue X1000).

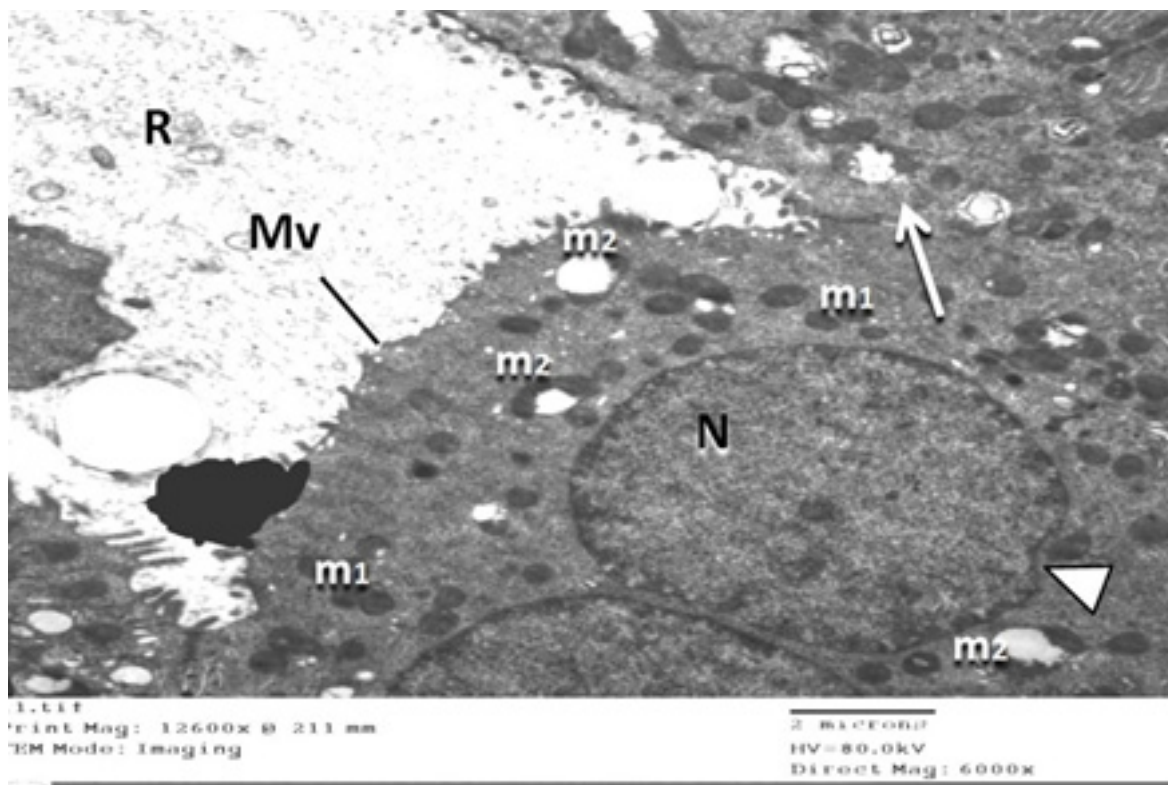


Fig. 9: An electron micrograph of a rat kidney of group II displaying a proximal convoluted tubular cell with the nucleus (N) showing indented nuclear membrane (arrowhead). The cell membrane is thick and irregular (white arrow), with loss of most of the apical microvilli (Mv). Mitochondria are markedly decreased, with some appearing normal (m1) while others are ballooned with loss of cristae (m2) (EM X6000).

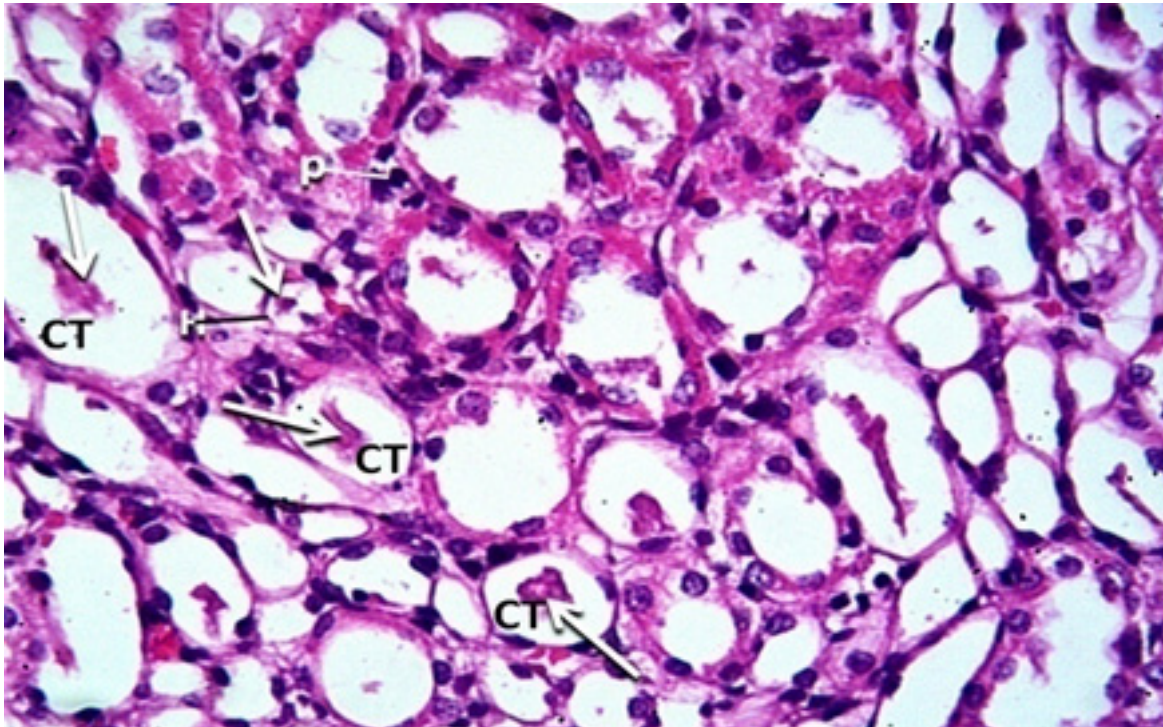


Fig. 10: A photomicrograph of a cross section of the renal medulla of a rat of group II showing loops of Henle (H) and collecting tubules (CT) showing marked atrophy with intra-luminal casts (white arrows) and nuclear pyknosis (p) of lining epithelial cells (Hx.&E.X400).

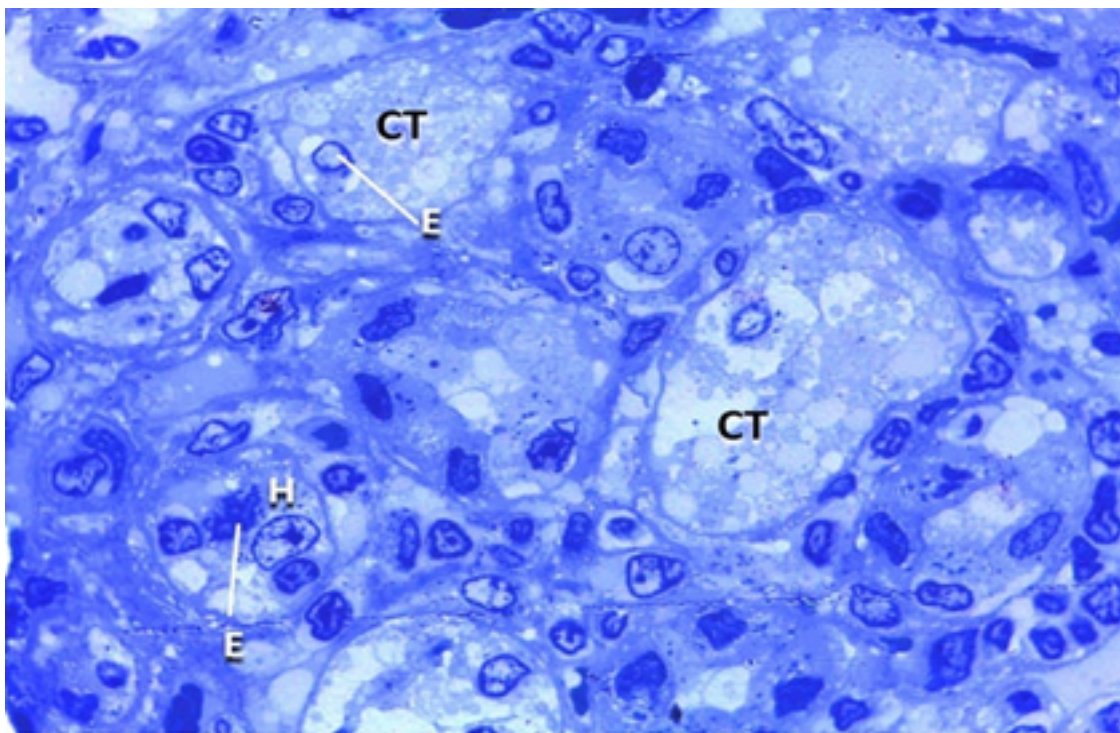


Fig. 11: A photomicrograph of a semithin section of the renal medulla of a rat of group II presenting completely degenerated epithelial lining of collecting tubules (CT) and the ascending limb of loop of Henle (H) with exfoliated cells into the lumen (E). There is marked infiltration of the interstitial tissue with fibroblasts (black arrows) and mononuclear cells (red arrows) (Toluidine blue X1000).

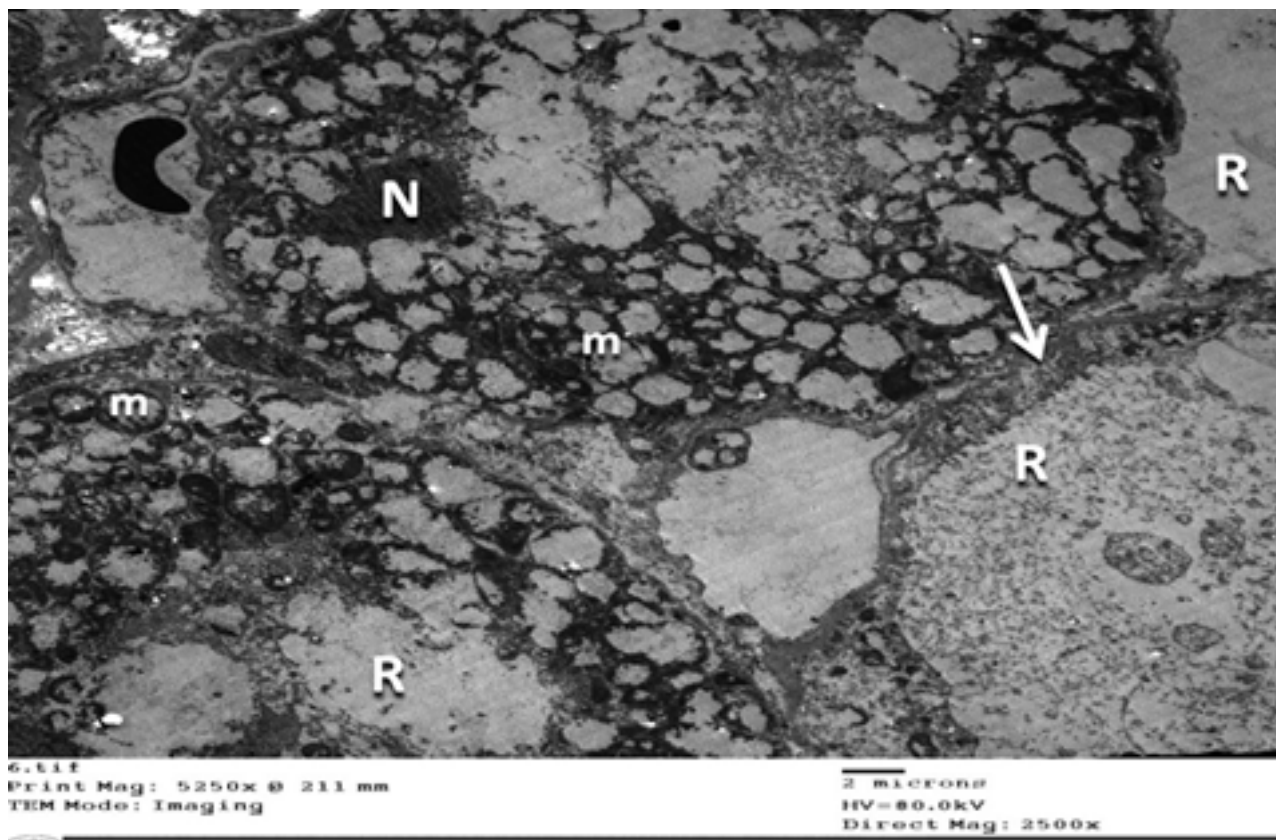


Fig. 12: An electron micrograph of a rat kidney of group II displaying the epithelial cells lining the ascending limb of loop of Henle, with pyknotic nuclei (N), extensive cytoplasmic rarefaction (R), damaged ballooned mitochondria (m) with complete loss of cristae, and markedly thick irregular basal cell membrane (white arrow) (EM X2500).

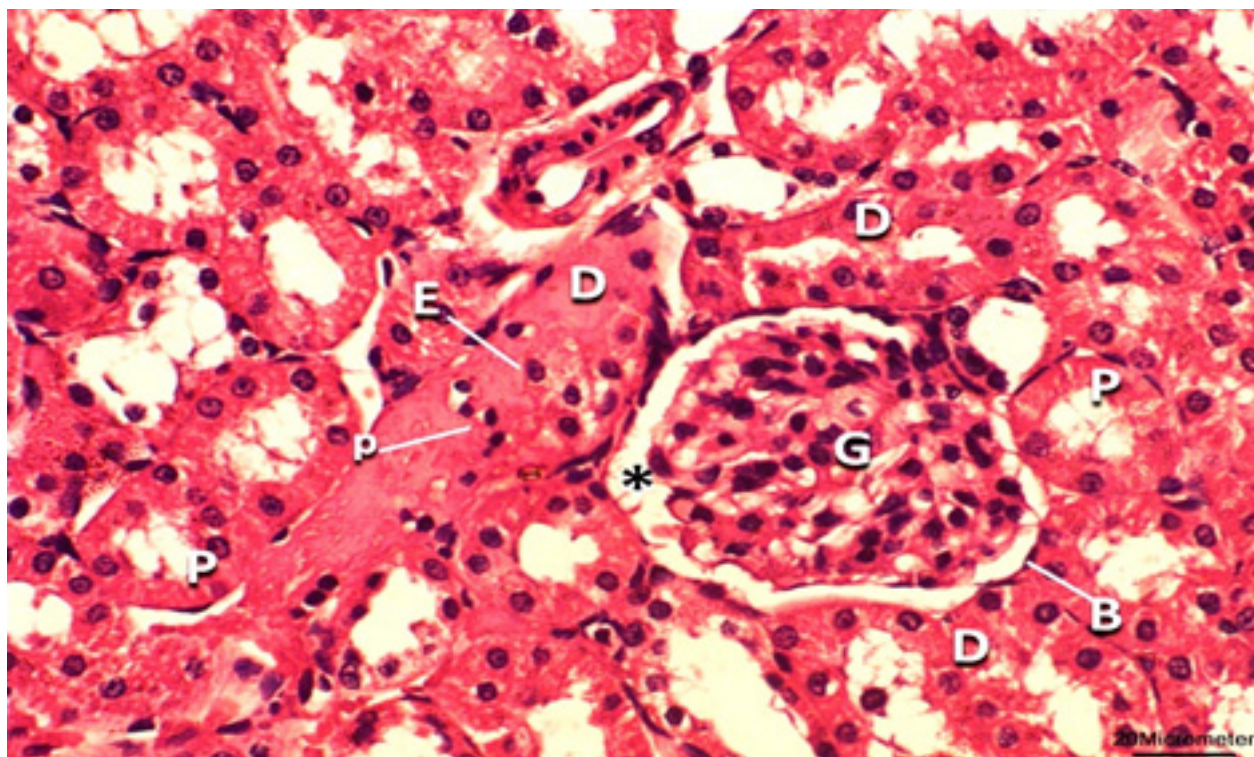


Fig. 13: A photomicrograph of a cross section of the renal cortex of a rat of group III (Cisplatin and erythropoietin pre-administration group) showing an apparently normal renal corpuscle formed of a dense rounded glomerulus (G) surrounded by a parietal layer of Bowman's capsule (B) with apparently normal urinary space (*). The proximal (P) and distal (D) convoluted tubules are apparently normal. Few exfoliated epithelial cells (E) and pyknotic nuclei are present (Hx.&E. X400).

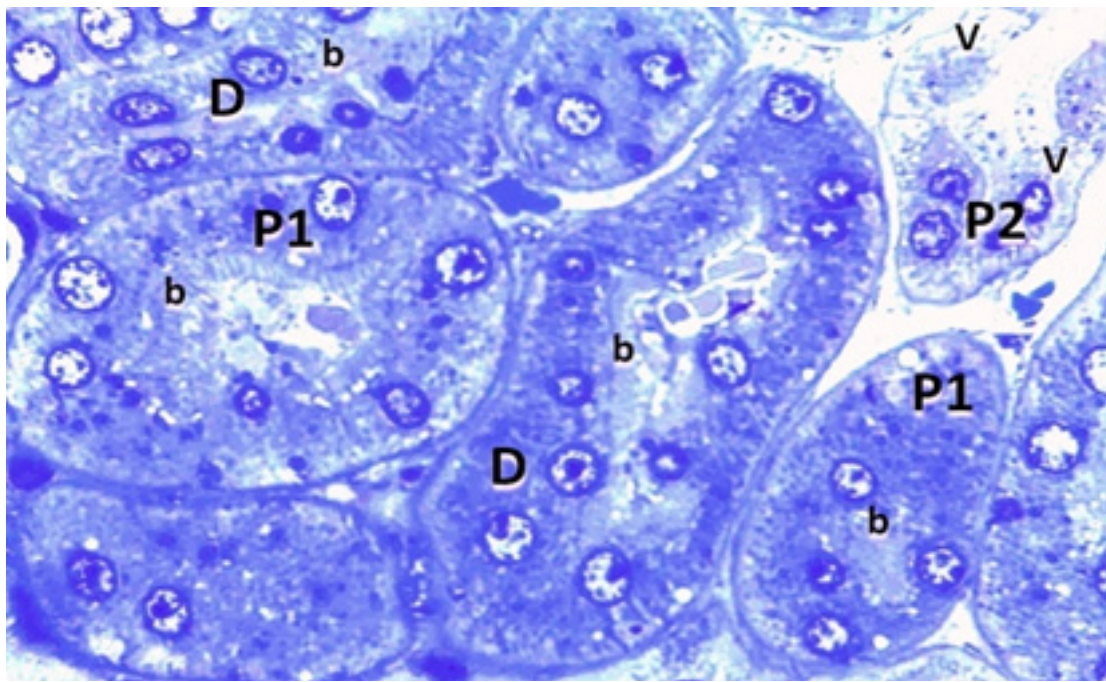


Fig. 14: A photomicrograph of a semithin section of the renal cortex of group III demonstrating apparently normal proximal (P1) and distal (D) convoluted tubules, with an intact apical brush border (b) in most of the proximal tubules. Few proximal tubules (P2) displayed cytoplasmic vacuolation (V) of the lining cells with loss of the apical brush border (Toluidine blue X1000).

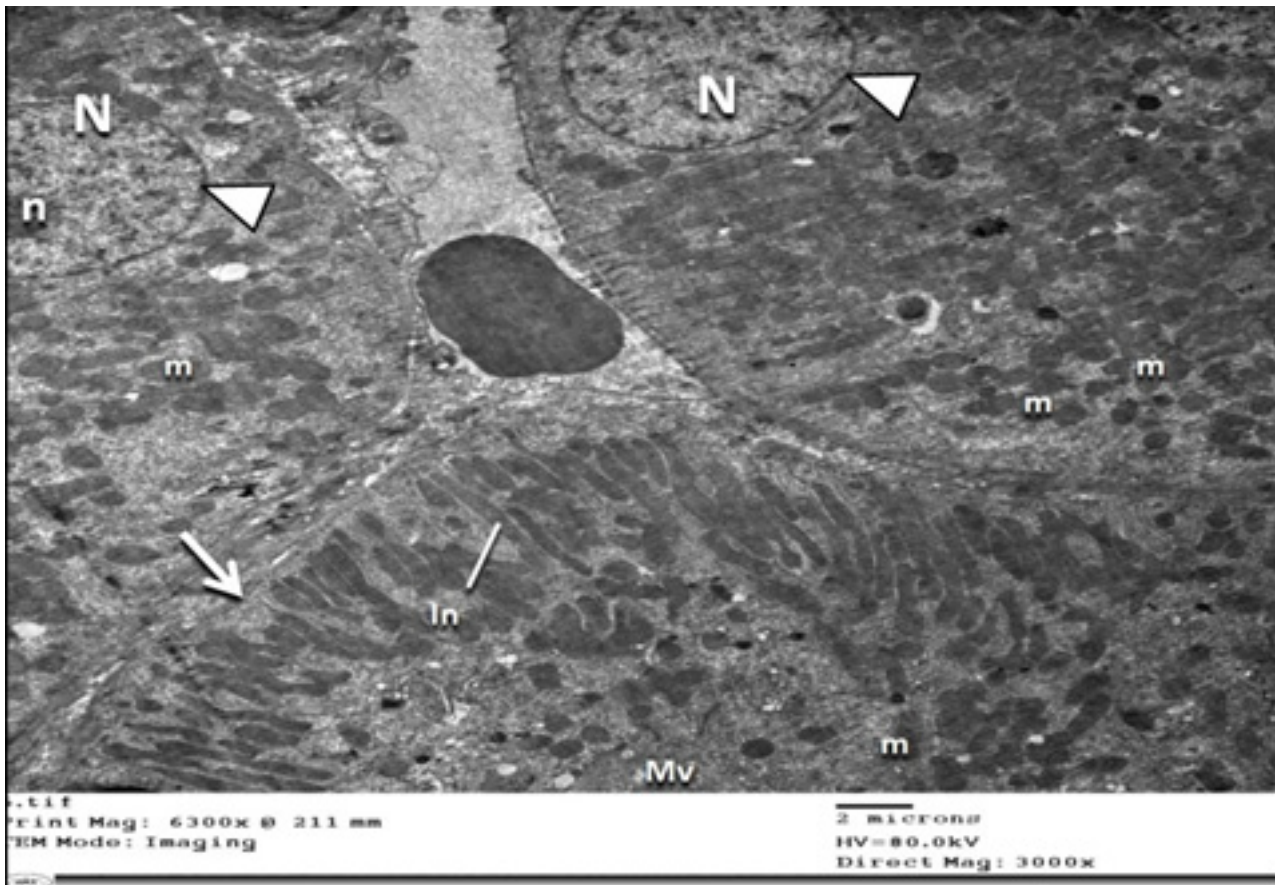


Fig. 15: An electron micrograph of a rat kidney of group III displaying cells of a proximal convoluted tubule. The cells show rounded heterochromatic nuclei (N) with prominent nucleoli (n) and intact nuclear envelop (arrowhead). There are numerous apparently normal mitochondria (m). The basolateral cell membrane is thin and regular (white arrow) with intact basal infoldings (In). The apical membrane shows preserved microvilli in some cells (red arrow) with loss of them in other cells (black arrow) (EM X 3000).

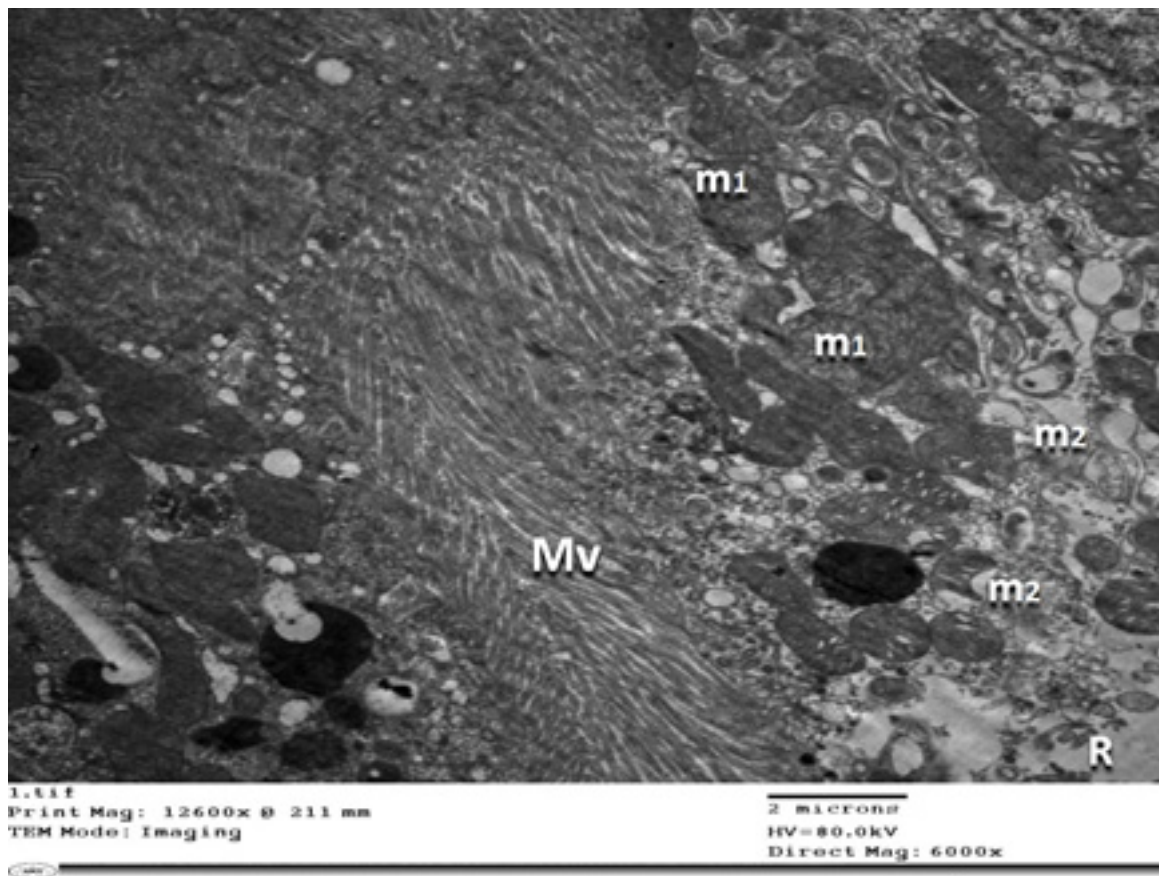


Fig. 16: An electron micrograph of a rat kidney of group III displaying a proximal convoluted tubular cell with intact apical microvilli (Mv). There is mild cytoplasmic rarefaction (R). Most of the mitochondria appeared normal (m1), while few of them appeared ballooned with damaged cristae (m2) (EM X6000).

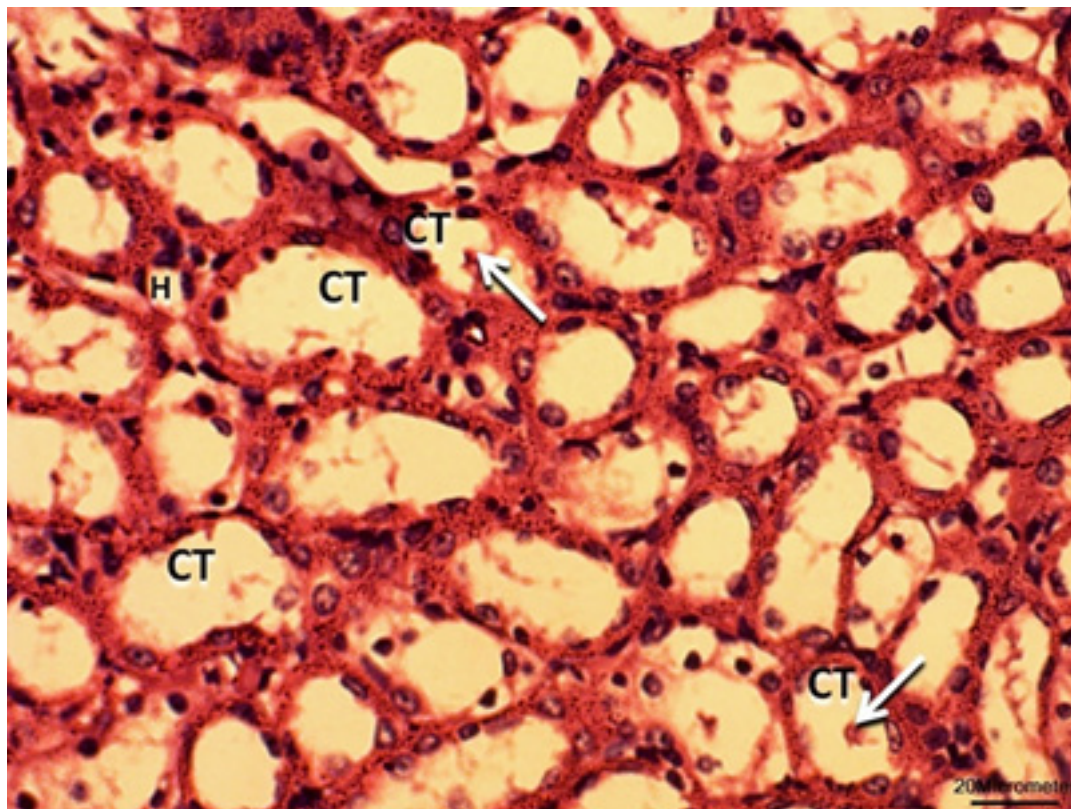


Fig. 17: A photomicrograph of a cross section of the renal medulla of a rat of group III showing apparently normal loops of Henle (H) and collecting tubules (CT). Few of them exhibited intra-luminal casts (white arrows) (Hx.&E. X400).

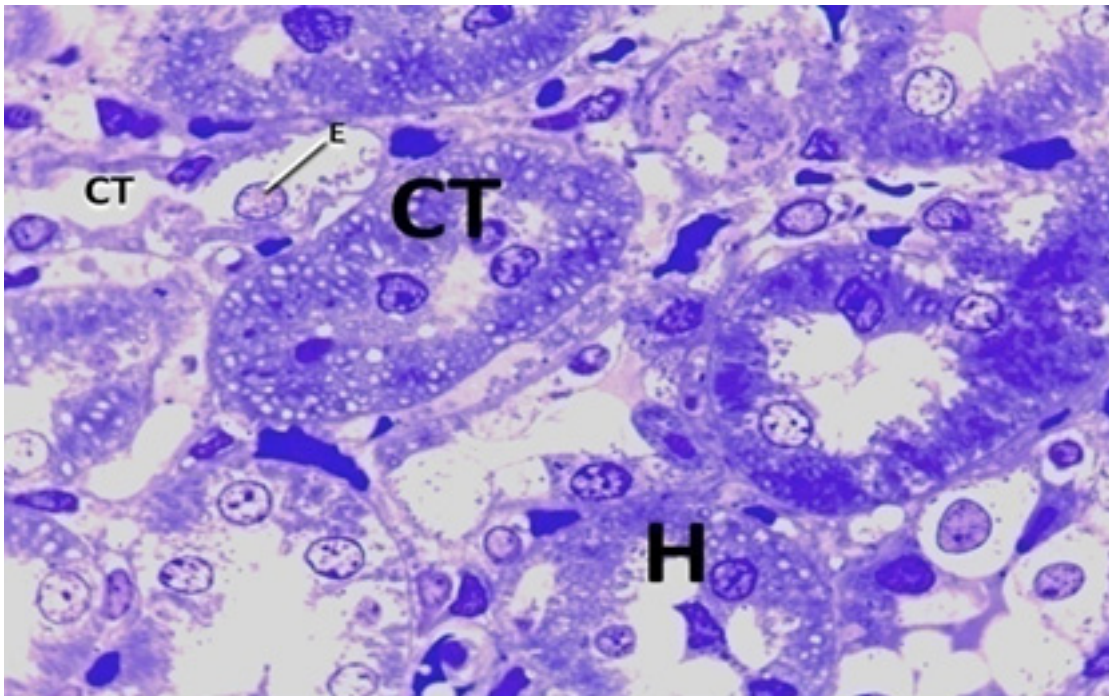


Fig. 18: A photomicrograph of a semithin section of the renal cortex of group III. Most of the collecting tubules are apparently normal (black CT), while few show damage of the lining epithelium (red CT). The ascending limb of loop of Henle (H) and collecting ducts display few exfoliated cells (E) (Toluidine blue X 1000).

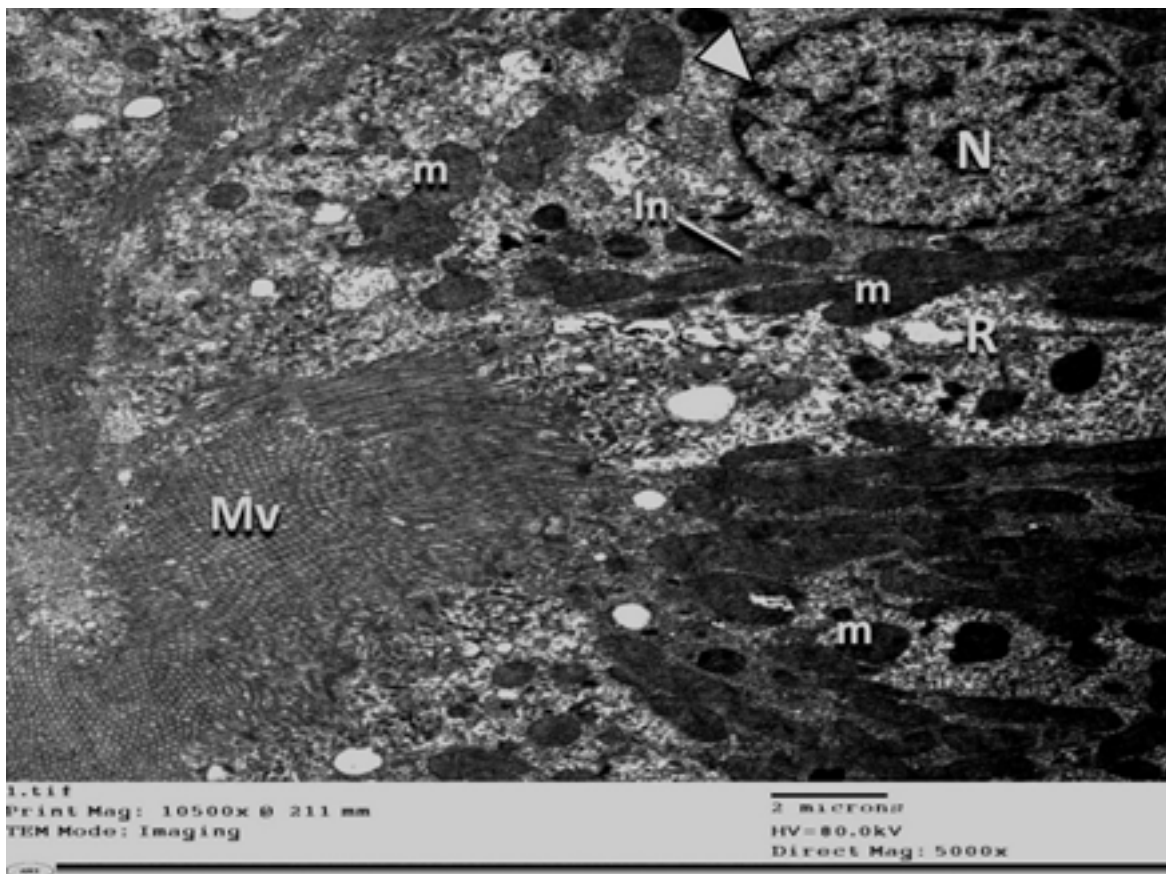


Fig. 19: An electron micrograph of the medulla of a rat kidney of group III displaying the epithelial lining cells of the ascending limb of loop of Henle. The cells contain heterochromatic nuclei (N) with intact nuclear envelop (arrowhead) and abundant apparently normal mitochondria (m). There is mild cytoplasmic rarefaction (R). The apical membrane shows numerous intact microvilli (Mv) (EM X5000).

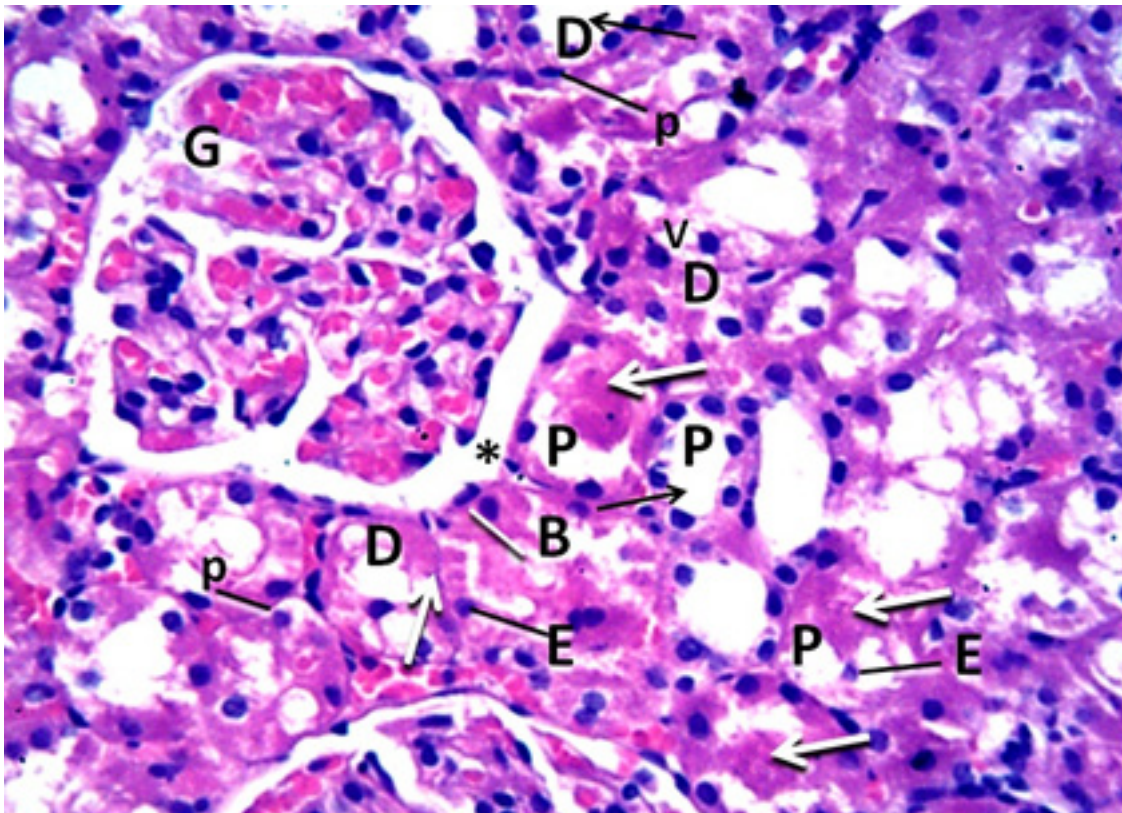


Fig. 20: A photomicrograph of a cross section of the renal cortex of a rat of group IV (Cisplatin and erythropoietin co-administration group) showing moderately shrunken and congested glomeruli (G) surrounded by a parietal layer of Bowman's capsule (B) with a mildly widened urinary space (*). Most of proximal (P) and distal (D) convoluted tubules are dilated (black arrows) and contain intraluminal casts (white arrow) with exfoliated epithelial cells (E). Lining cells display pyknotic nuclei (p) and cytoplasmic vacuolation (v) (Hx.&E. X400).

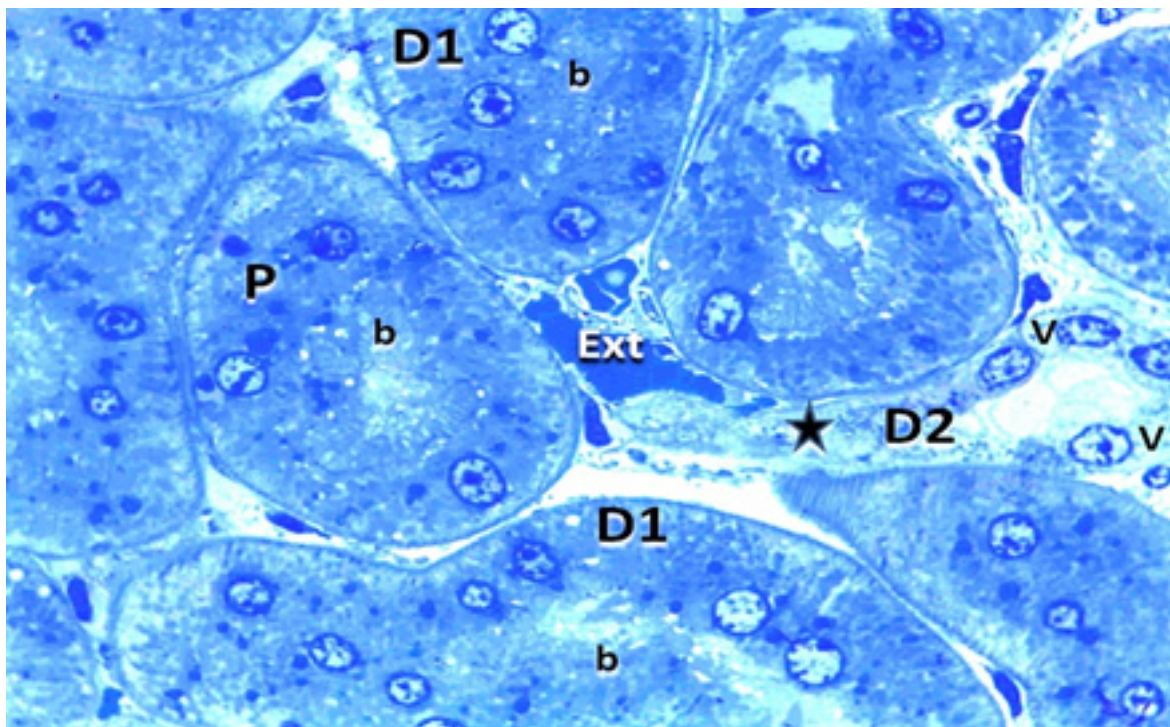


Fig. 21: A photomicrograph of a semithin section of the renal cortex of group IV demonstrating apparently normal proximal (P) and distal (D1) convoluted tubules with intact apical brush border (b) in the proximal tubules. Some of the distal tubules (D2) are collapsed (star) and their lining cells display cytoplasmic vacuolation (V). Interstitial tissue shows extravasated blood (Ext) (Toluidine blue X1000).

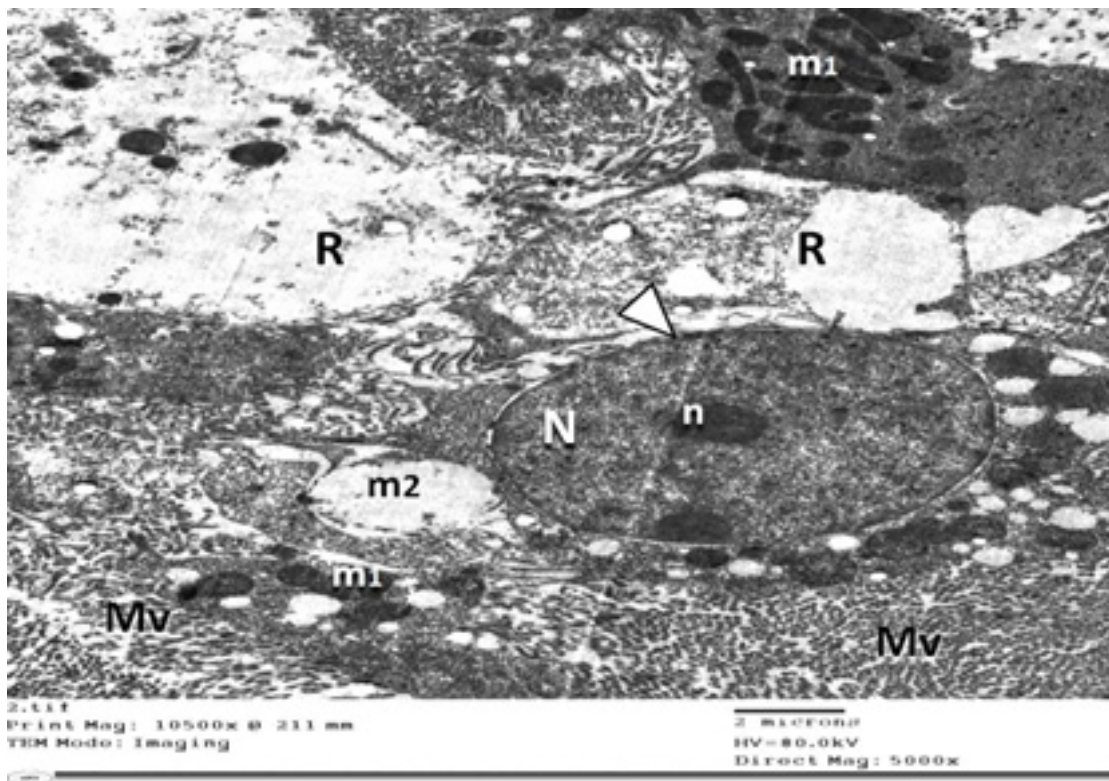


Fig. 22: An electron micrograph of a rat kidney of group IV displaying a proximal convoluted tubular cell with a heterochromatic nucleus (N) containing a prominent nucleolus (n) and intact nuclear envelop (arrowhead). The apical membrane shows partially damaged microvilli (Mv). The cytoplasm displays marked cytoplasmic rarefaction (R), with some mitochondria (m1) appearing normal while others appear ballooned with damaged cristae (m2) (EM X5000).

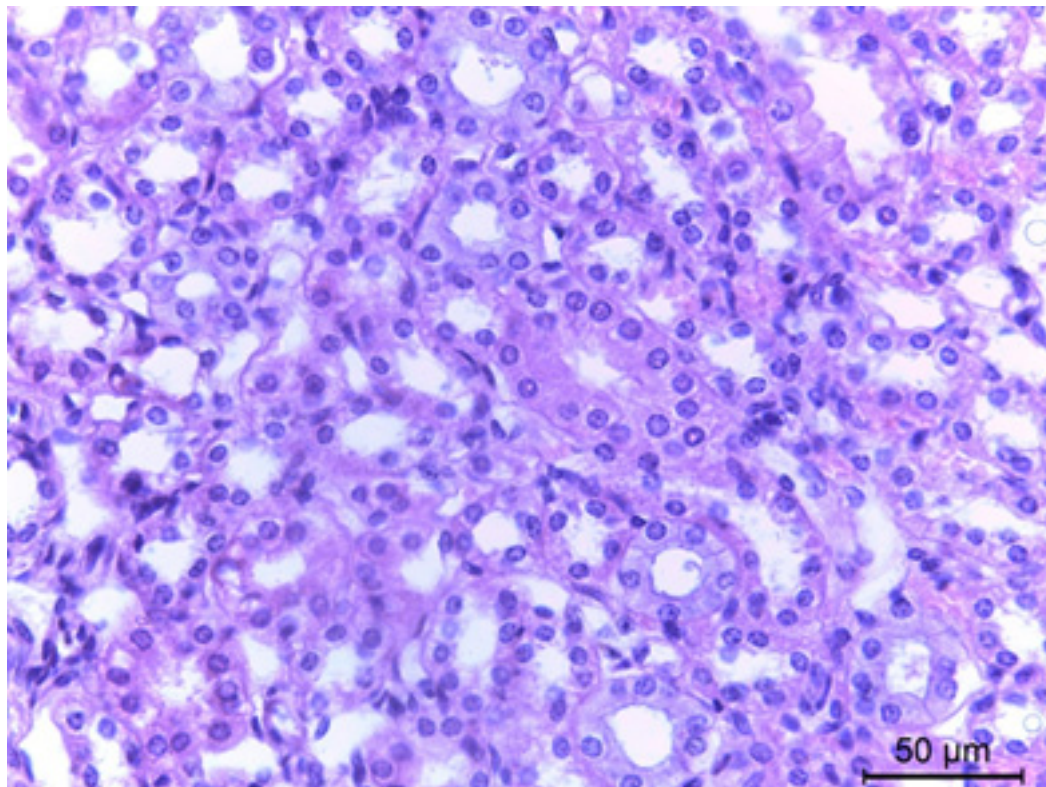


Fig. 23: A photomicrograph of a cross section of the renal medulla of group IV showing apparently normal loops of Henle (H) and collecting tubules (CT), with few intra-luminal casts (white arrows) and pyknotic nuclei (p) (Hx.&E. X400).

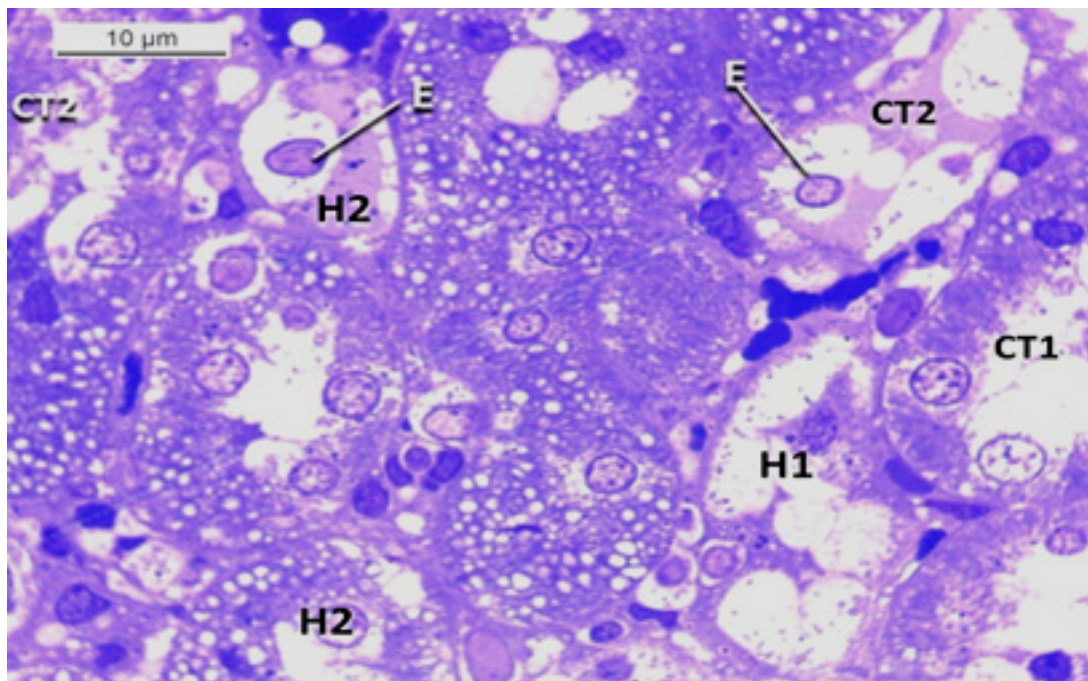


Fig. 24: A photomicrograph of a semithin section of the renal medulla of group IV presenting apparently normal epithelial lining of collecting tubules (CT1) and the ascending limb of loop of Henle (H1). Some of them appeared collapsed and degenerated (CT2, H2) with exfoliated cells (E) into their lumina (Toluidine blue X1000).

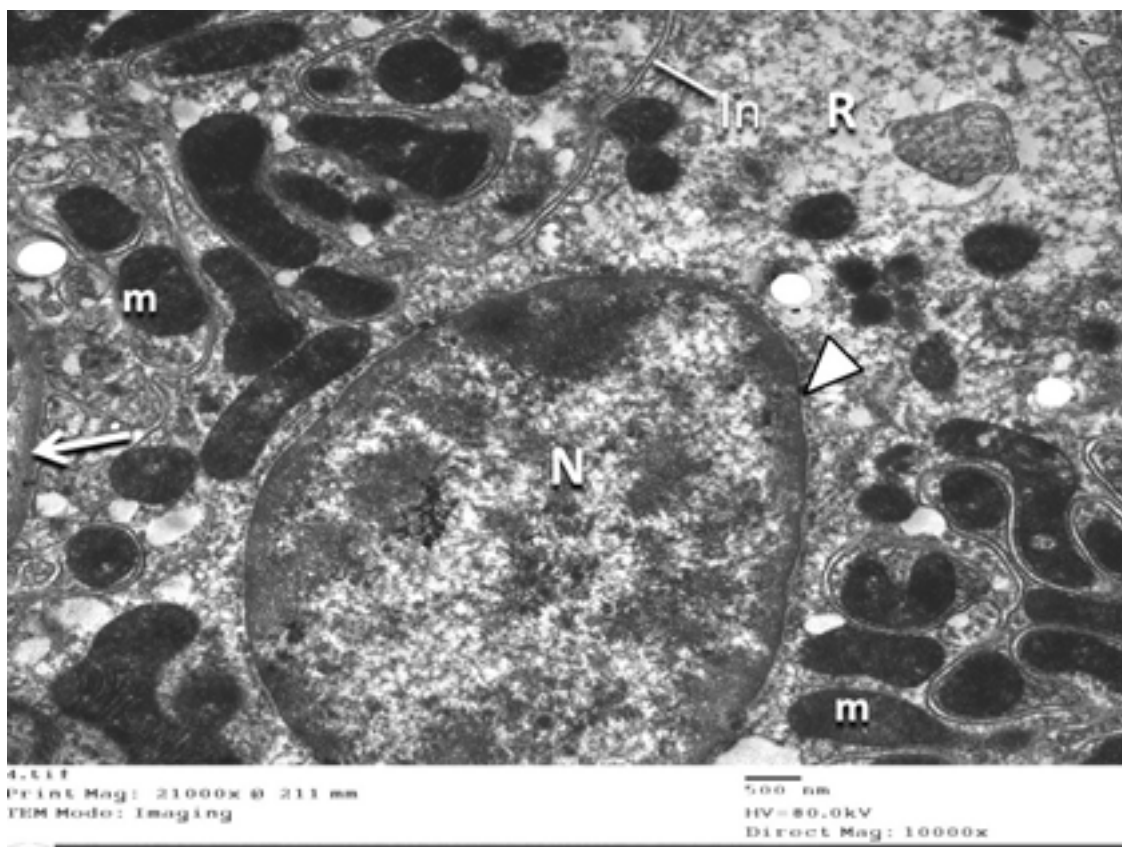


Fig. 25: An electron micrograph of the medulla of a rat kidney of group IV displaying an epithelial lining cell of the ascending limb of loop of Henle. The nucleus (N) is apparently normal with heterochromatin and intact nuclear envelop (arrowhead). The cytoplasm shows mild rarefaction, with numerous apparently normal mitochondria (m) and intact basal infoldings (In). The basolateral membrane is thin and uniform (white arrow) (EM X10000).

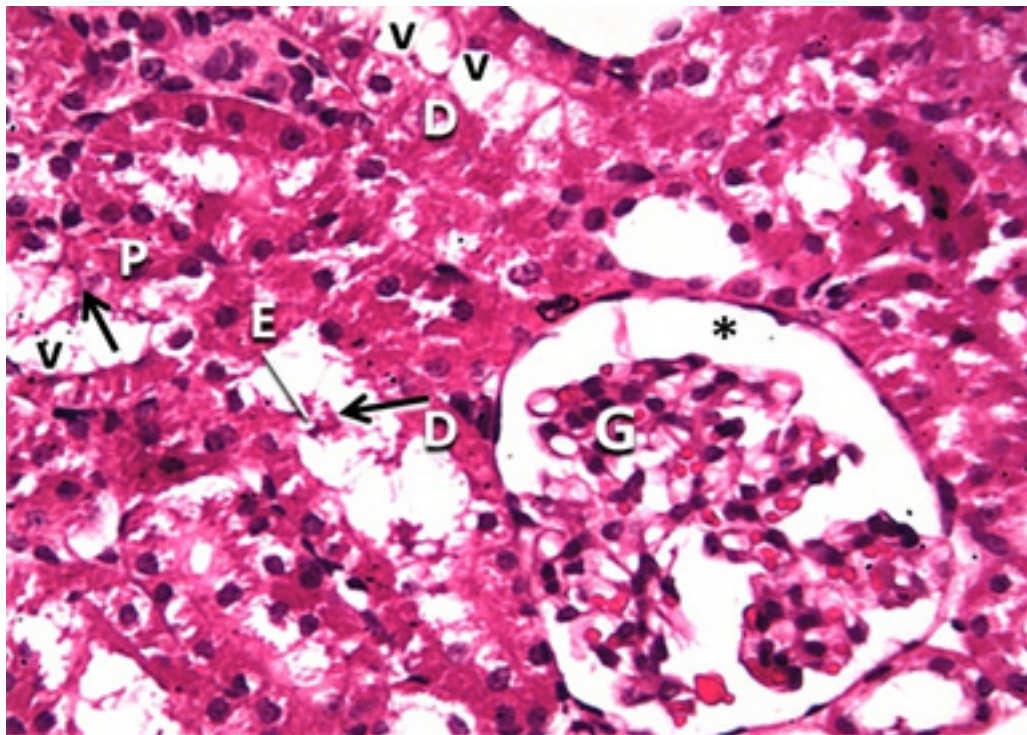


Fig. 26: A photomicrograph of a cross section of the renal cortex of a rat of group V (Cisplatin and erythropoietin post-administration group) showing shrunken glomeruli (G) with a widened urinary space (*). Most of proximal (P) and distal (D) convoluted tubules are widened and irregular, with destroyed lining vacuolated epithelium (v). Their lumina contain intraluminal casts (black arrows) and exfoliated cells (E) (Hx.&E. X400).

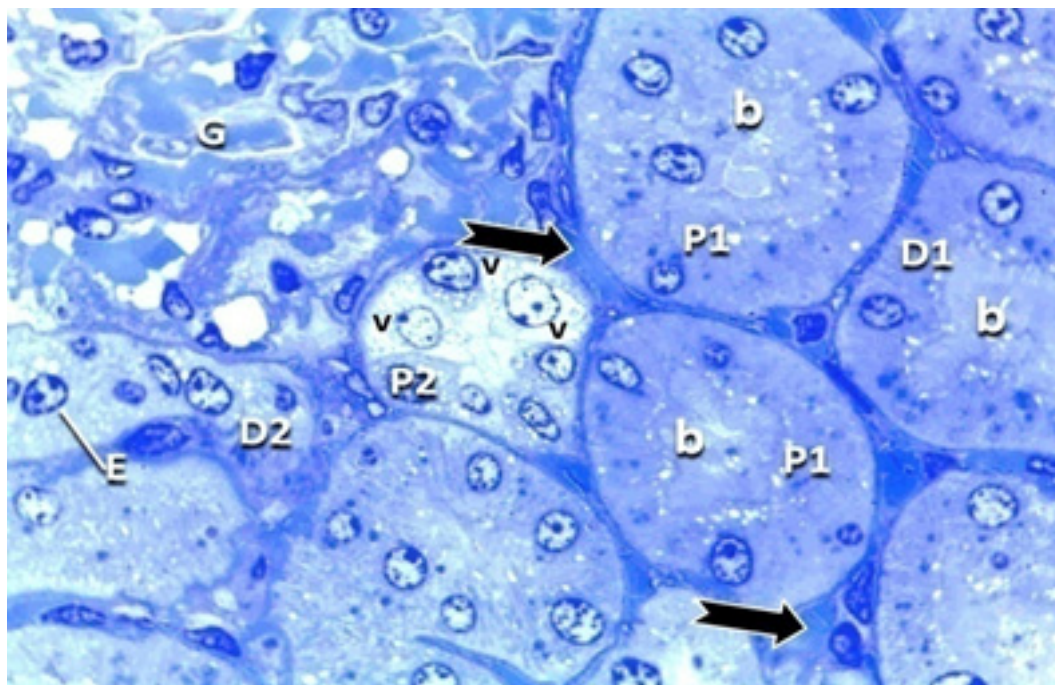


Fig. 27: A photomicrograph of a semithin section of the renal cortex of group V demonstrating apparently normal glomerulus (G), proximal (P1) and distal (D1) convoluted tubules with intact apical brush border in the proximal tubules (b). Some tubules (P2, D2) exhibited cytoplasmic vacuolation (V) and epithelial cell exfoliation into the tubular lumen (E). Interstitial tissue shows exudation (notched black arrows) and infiltration by mononuclear cells (red arrows) (Toluidine blue X1000).

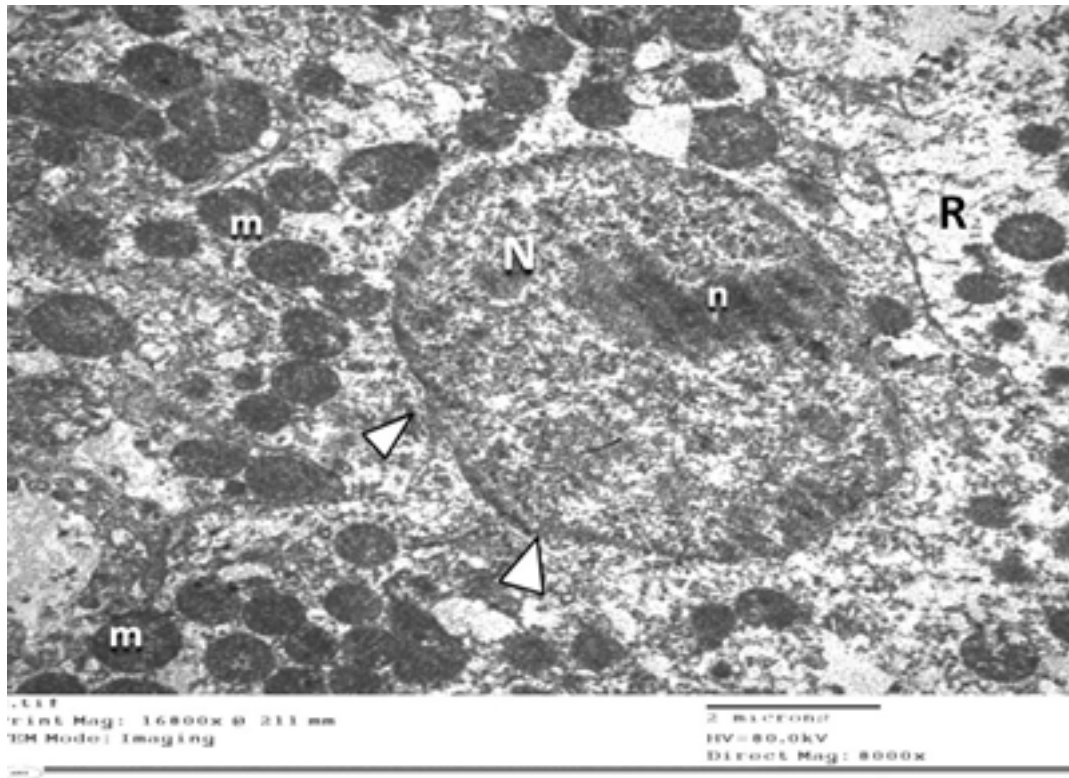


Fig. 28: An electron micrograph of the cortex of a rat kidney of group V displaying a proximal convoluted tubular cell in which the nucleus (N) displayed an ill-defined nucleolus (n) and a disrupted nuclear envelop (arrowhead). The cytoplasm shows marked rarefaction (R) and contains many apparently normal mitochondria (m) (EM X8000).

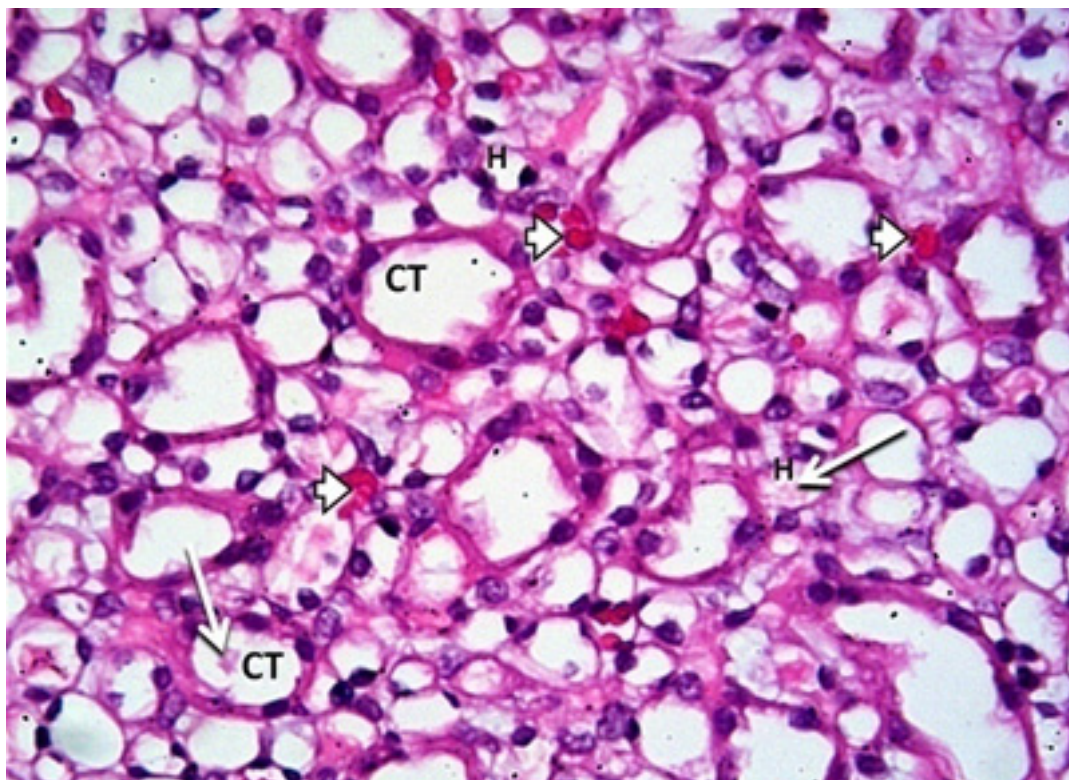


Fig. 29: A photomicrograph of a cross section of the renal medulla of group V showing loops of Henle (H) and collecting tubules (CT) with intra-luminal casts (long white arrows). Congested capillaries exist among the tubules (short white arrows) (Hx.&E. X400).

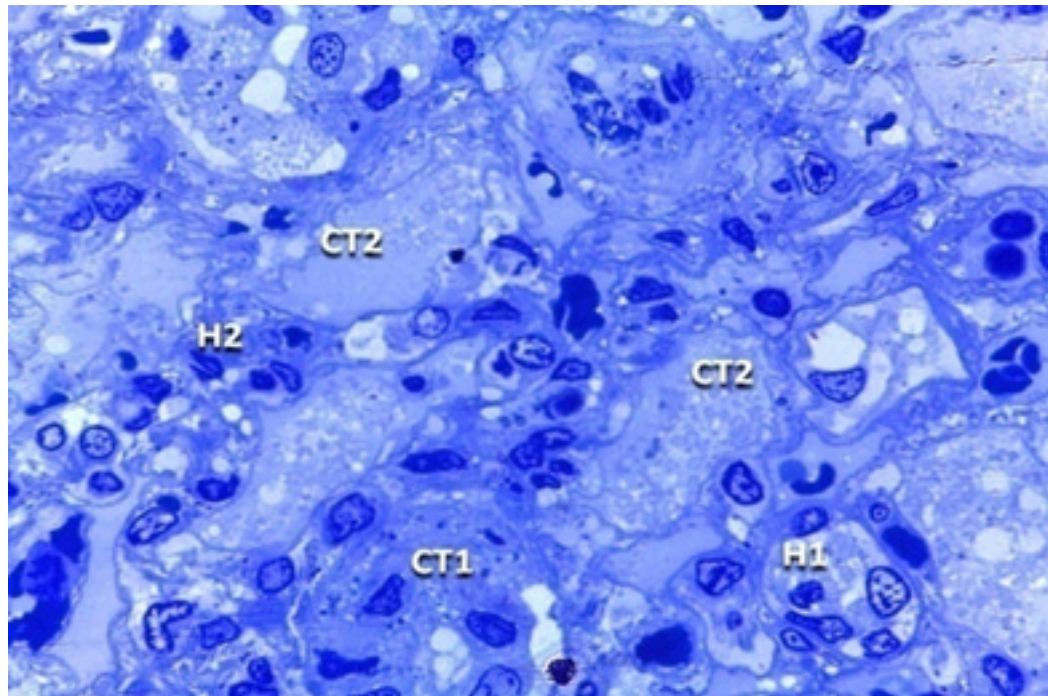


Fig. 30: A photomicrograph of a semithin section of the renal medulla of group V. Some of the collecting tubules (CT1) and ascending limbs of loops of Henle (H1) appear mostly normal, while others (CT2 and H2) are collapsed and are lined by degenerated cells (Toluidine blue X1000).

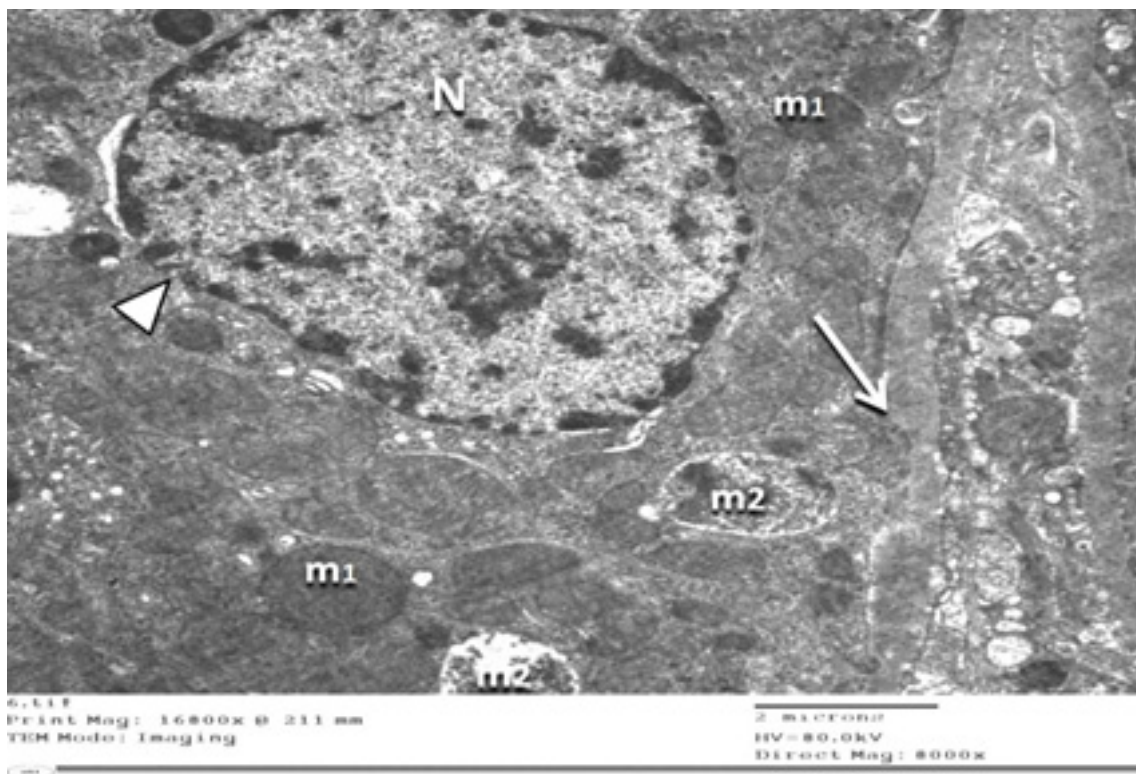
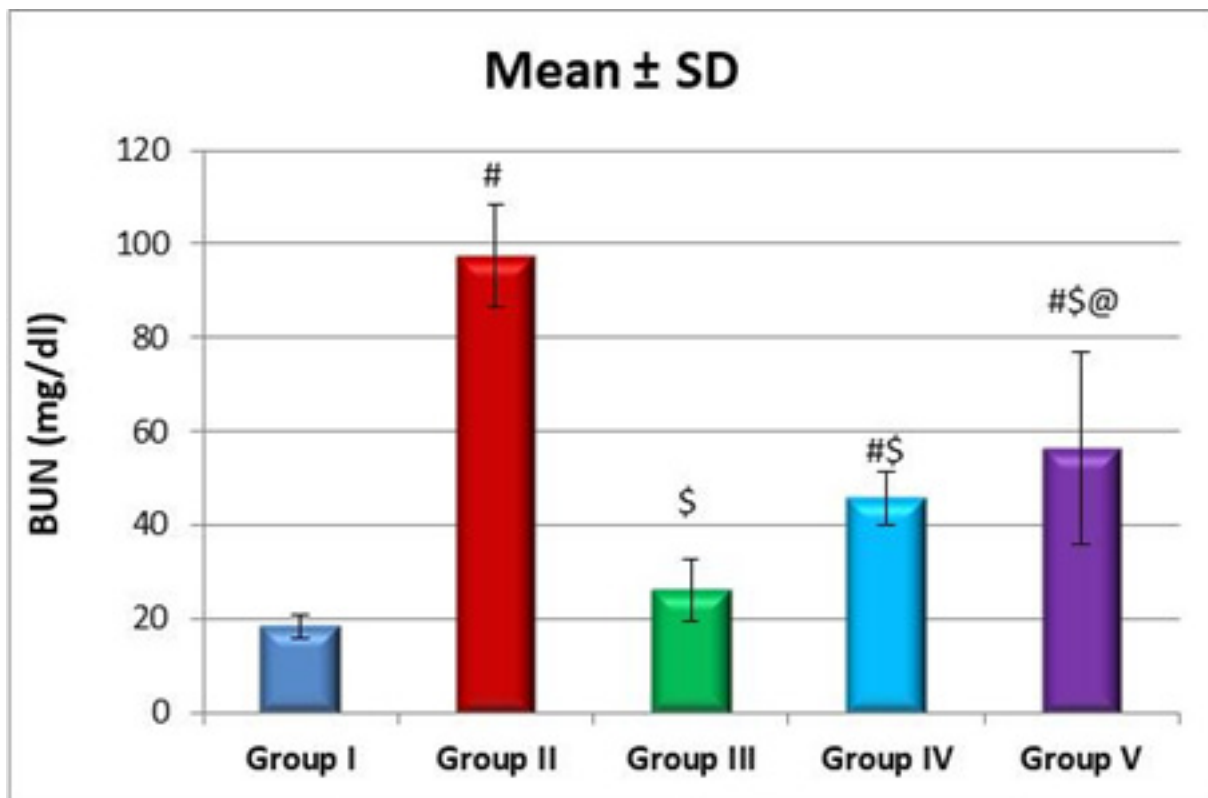


Fig. 31: An electron micrograph of the medulla of a rat kidney of group V displaying an epithelial lining cell of the ascending limb of loop of Henle in which the nucleus (N) displays peripherally clumped chromatin and a disrupted nuclear envelop (arrowhead). The basal cell membrane is thick and irregular (white arrow). Some mitochondria (m1) are apparently normal while others are ballooned with lost cristae (EM X8000).

	Group I		Group II		Group III		Group IV		Group V	
	Mean	SD	Mean	SD	Mean	SD	Mean	SD	Mean	SD
BUN mg/dl	18.48	2.65	97.38	10.93	26.24	6.7	45.72	5.67	56.62	20.51
<i>P-values</i>										
G I vs. G II	<0.0001 (S)									
G I vs. G III	0.806 (NS)									
G I vs. G IV	0.008 (S)									
G I vs. G V	<0.0001 (S)									
G II vs. G III			<0.0001 (S)							
G II vs. G IV			<0.0001 (S)							
G II vs. G V			<0.0001 (S)							
G III vs. G IV					0.080 (NS)					
G III vs. G V							0.003 (S)			
G IV vs. G V							0.549 (NS)			

Fig. 32: A table demonstrating mean values of blood urea nitrogen (BUN) among different study groups.

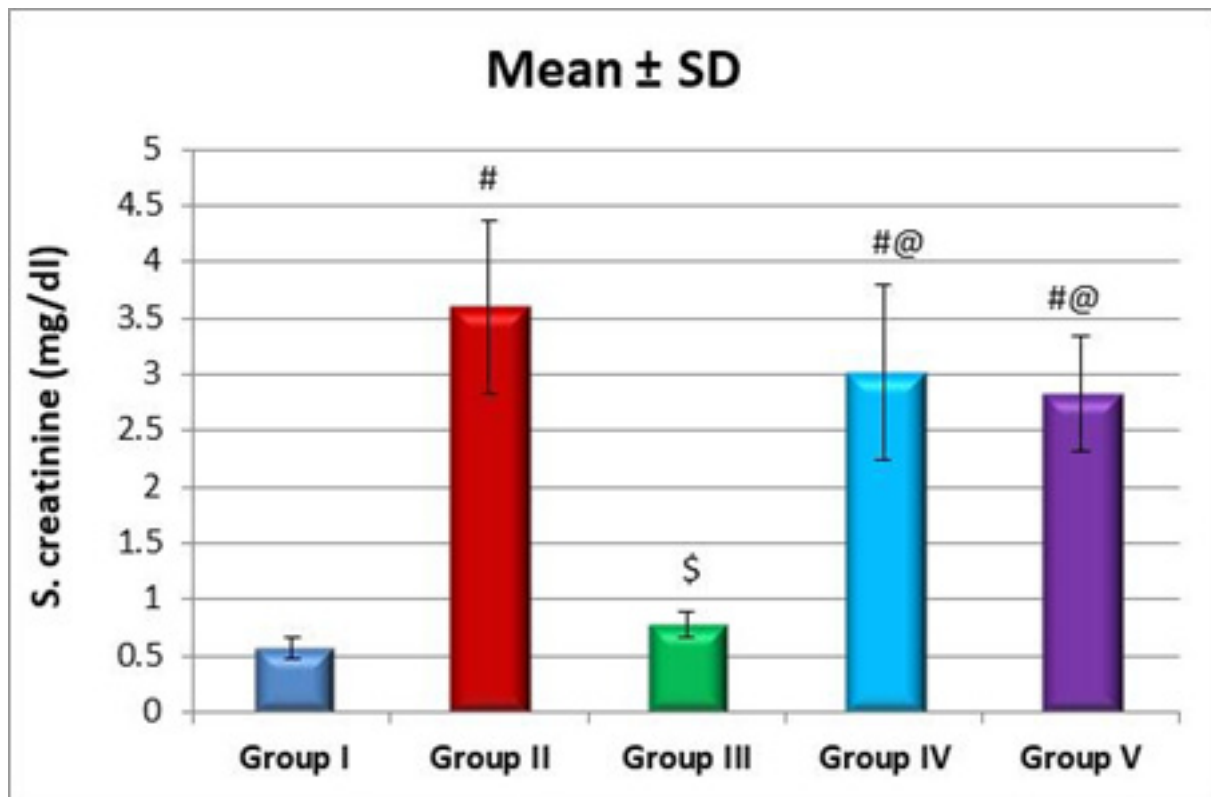


Significant from group I, \$ significant from group II, @ significant from group III

Fig. 33: Histogram illustrating mean values of blood urea nitrogen (BUN) obtained from the different groups of the examined animals.

	Group I		Group II		Group III		Group IV		Group V	
	Mean	SD	Mean	SD	Mean	SD	Mean	SD	Mean	SD
<i>P-values</i>										
G I vs. G II	<0.0001 (S)									
G I vs. G III	0.976 (NS)									
G I vs. G IV	<0.0001 (S)									
G I vs. G V	<0.0001 (S)									
G II vs. G III			<0.0001 (S)							
G II vs. G IV			0.467 (NS)							
G II vs. G V			0.207 (NS)							
G III vs. G IV					<0.0001 (S)					
G III vs. G V					<0.0001 (S)					
G IV vs. G V							0.980 (NS)			

Fig. 34: A table demonstrating mean values of serum creatinine among different groups.



Significant from group I, \$ significant from group II, @ significant from group III

Fig. 35: Histogram illustrating mean values of serum creatinine obtained from the different groups of the examined animals.

DISCUSSION

In the present work, cisplatin administration exerted marked histological alterations in the renal tissue (cortex and medulla) in the form of shrunken and collapsed glomeruli, atrophic and degenerated tubules, mitochondrial damage, nuclear pyknosis, cytoplasmic vacuolation, loss of apical microvilli and basal infoldings, extravasated blood and accumulation of inflammatory exudate in the interstitial tissue. These alterations were more evident in the renal cortex. Similar findings were observed by **Sabine et al., 2011**; **Guo et al., 2018** and **Sonoda et al., 2019**, who stated that cisplatin-induced marked atrophy in the tubular cells of the renal cortex. The authors attributed such changes to oxidative stress and glomerular hypoperfusion, with subsequent reduction of blood flow through the peritubular capillaries, leading to tubular ischemia and atrophy. The more marked pathology in the renal cortex could be explained on the basis of the fact that renal cortex receives about 90% of the renal blood flow as documented by **Widmaier et al. (2014)**, thus delivering a higher concentration of cisplatin to the renal cortex and tubular cells. **Schrier (2007)** and **Legrand et al. (2008)** attributed the necrotic changes to acute ischaemia and microvascular disorder caused by an imbalance between vasoconstrictors (especially endothelin-1) and vasodilators (especially nitric oxide), leading to decreased renal oxygen supply. According to **Schrier (2007)**, cells of the proximal convoluted tubules suffered extensive necrosis following clamping of renal vessels for 45 to 60 minutes. Another possible mechanism is that reported by **Basile et al. (2012)**, who pointed out that adenosine released from catabolised nucleotides of necrotic cells acts as a powerful renal vasoconstrictor via activating A1 receptors, augmenting the ischemia and setting a vicious circle of the renal tubular cell damage. **Flávio et al., 2007**; **Haram et al., 2008**; **Francescato et al., 2009** and **Sánchez-González et al., 2011** reported that cisplatin injection induces endothelial injury with subsequent vasoconstriction and vascular thrombosis, ending in decreased renal plasma flow. The authors added that, endothelial damage augments expression of molecules that favour leukocyte binding to the endothelium. **Francescato et al. (2018)** elucidated that cisplatin injection produces ROS that activate inflammatory pathways that include activated protein kinases. **Volarevic et al. (2019)** reported cisplatin to increase neutrophil and macrophage recruitment and to augment the generation of tumor necrosis factor α and interleukin-1 in the renal cortex and medulla, which in turn enhance necrotic and apoptotic consequences in the tubular epithelial cells.

In the present study, mitochondria exhibited the most severe form of injury in response to cisplatin administration. This goes hand in hand with **Lomeli et al. (2017)**, who pointed out that cisplatin injection induced marked mitochondrial damage in rat hippocampal neurons, while the other organelles exhibited a less severe injury.

The mitochondrial damage induced by ischemia and hypoxia was explained earlier by **Feldkamp et al. (2005)** who attributed the damage to an increase in the inner mitochondrial membrane permeability, with subsequent influx of Na ions leading to mitochondrial swelling and fragmentation. The nuclear degenerative and necrotic changes detected in the current study could be explained as a consequence of blockage of replication and transcription of nuclear DNA, which is induced by cisplatin as documented by **Marullo et al. (2013)**.

In the current work, cisplatin administration markedly increased blood urea and serum creatinine levels. This was in accordance with **Sonoda et al. (2019)** who reported that injection of cisplatin was accompanied by marked increase in blood urea nitrogen and serum creatinine 24 hours after cisplatin administration. **Vickers et al. (2004)** and **Perše and Haler (2018)** stated that cisplatin disturbs genes involved in renal functions such as biochemical pathways related to creatinine biosynthesis and gene expression consequences related to drug metabolism and detoxification. The present study showed that administration of erythropoietin markedly ameliorated all histological and biochemical alterations especially when injected prior to cisplatin administration. This was in agreement with **Grasso et al. (2004)**; **Hanlon et al. (2005)** and **Ifeanyi and Uzoma (2016)** who stated that erythropoietin could ameliorate overproduction of reactive oxygen species in diabetic nephropathy and in rats with severe glomerulonephritis. **Souma et al. (2015)** admitted that erythropoietin receptors are located in the proximal tubules, mesangium and collecting duct cells of the kidney. They added that these receptors are amenable for upregulation in pathological conditions such as renal ischaemia, but their affinity is lower than that in hypoxic states that stimulate erythropoiesis. So, higher doses of erythropoietin are required to induce cytoprotection compared with those needed to stimulate erythropoiesis. **La Ferla (2002)**; **Wenger and Hoogewijs (2010)**; **Kishore et al. (2011)**; **Jelkmann and Elliott (2013)**; **Rivkin, et al. (2016)** and **Ozkurt et al. (2018)** pointed out that TNF- α suppresses erythropoietin synthesis by the renal fibroblasts, thus causing normocytic anemia (anemia of chronic diseases). So, treatment with synthetic erythropoietin has a beneficial role in management of acute and chronic nephropathy.

CONCLUSION

The present work confirms that treatment with erythropoietin could ameliorate the pathological changes and biochemical derangements induced by chemotherapy with cisplatin, and the benefits of erythropoietin are more marked when it is administered prior to cisplatin administration.

CONFLICT OF INTEREST

There are no conflicts of interest.

REFERENCES

1. **Basile D.P.; Anderson M.D. and Sutton T.A. (2012):** Pathophysiology of Acute Kidney Injury. *Compr Physiol.*, 2(2): 1303–1353.
2. **Caoa, X.; Nieb, X.; Xionga, S.; Caoa, L.; Wua, Z.; Moorea, P.K. and Biana, J.S. (2018):** Renal protective effect of polysulfide in cisplatin-induced nephrotoxicity. *Redox Biology*, 15: 513–521.
3. **De Nicola, L. and Zoccali, C. (2016):** Chronic kidney disease prevalence in the general population heterogeneity and concerns. *Nephrol. Dial. Transplant.*, 31: 331–335.
4. **Del Vecchio, L. and Zuccala, A. (2017):** Erythropoiesis stimulating agents and nephroprotection: is there any room for new trials? *Nephrol. Dial. Transplant.* 32: 211–214.
5. **Feldkamp T.; Kribben A. and Weinberg J.M. (2005):** Assessment of mitochondrial membrane potential in proximal tubules after hypoxia-reoxygenation. *Am J Physiol Renal Physiol.*, 288 (6): 1092-1102.
6. **Francescato, H.D.C.; Costa, R.S.; Silva, G.C.A. and Coimbra, T.M. (2009):** Treatment with a p38 MAPK inhibitor attenuates cisplatin nephrotoxicity starting after the beginning of renal damage. *Life Sci.*, 84: 590-597.
7. **Francescato, H.D.C.; Almeida, L.F. Reis, N.G.; Faleiros, C.M.; Papoti, M.; Costac, R.S. and Coimbra, T.M. (2018):** Previous Exercise Effects in Cisplatin- Induced Renal Lesions in Rats. *Kidney Blood Press. Res.*, 43: 582-593.
8. **Flávio, A.G.C.; Cunha, F.Q.; Francescato, H.D.C.; Soares, T.J.; Costa, R.S.; Barbosa, J. and Coimbra, F. (2007):** TM:ATP-sensitive potassium channel blockage attenuates cisplatin-induced renal damage. *Kidney Blood Press. Res.*, 30: 289-298.
9. **Grasso, G.; Sfacteria, A.; Cerami, A. and Brines, M. (2004):** Erythropoietin as a tissue-protective cytokine in brain injury: what do we know and where do we go? *Neuroscientist.*, 10(2): 93-98.
10. **Guo Y., Wang M., Mou J., Zhao Z., Yang J., Zhu F., Guangchang P., Han Z., Wang Y., Gang X., Zeng R. and Yao Y. (2018):** Pretreatment of Huaiqihuang extractum protects against cisplatin-induced nephrotoxicity. *Scientific Reports*, 8(1): 33-37
11. **Hanlon, P.R.; Fu, P.; Wright, G.L.; Steenbergen, C.; Arcasoy, M.O. and Murphy, E. (2005):** Mechanisms of erythropoietin-mediated cardioprotection during ischemia-reperfusion injury: role of protein kinase C and phosphatidylinositol 3-kinase signaling. *FASEB J.*, 19(10): 1323-1325.
12. **Hanigan, M.H. and Devarajan, P. (2003):** Cisplatin nephrotoxicity: molecular mechanisms. *Cancer Ther.*, (1): 47-61.
13. **Haram, P.M.; Kemi, O.J. and Wisloff, U. (2008):** Adaptation of endothelium to exercise training: insights from experimental studies. *Front Biosci.*, 13: 336-346.
14. **Harpur, E.; Ennulat, D. and Hoffman. D. (2011):** “Biological qualification of biomarkers of chemical-induced renal toxicity in two strains of male rat,” *Toxicological Sciences*, 122(2): 235–252.
15. **Ifeanyi, O.E. and Uzoma, O.G. (2016):** Erythropoietin and Kidney Diseases: A Review. *J. Biol. Chem. Research*, 33 (2): 760-792.
16. **Jelkmann, W. And Elliott, S. (2013):** Erythropoietin and the vascular wall: the controversy continues. *Nutr. Metab. Cardiovasc. Dis.*, 23: 37-43.
17. **Kishore, R.; Tkebuchava, T.; Sasi, S.P.; Silver, M.; Gilbert, H.Y.; Yoon, Y.S.; Park, H.Y.; Thorne, T.; Losordo, D.W. and Goukassian, D.A. (2011):** Tumor necrosis factor-alpha signaling via TNFR1/p55 is deleterious whereas TNFR2/p75 signaling is protective in adult infarct myocardium. *Adv. Exp. Med. Biol.*, 691: 433-448.
18. **La Ferla, K.; Reimann, C.; Jelkmann, W. and Hellwig-Burgel, T. (2002):** Inhibition of erythropoietin gene expression signaling involves the transcription factors GATA-2 and NF-kappaB. *FASEB J.*, 16: 1811-1813.
19. **Legrand, M.; Mik, E.G.; Johannes, T.; Payen, D. and Ince, C. (2008):** Renal Hypoxia and Dysoxia after Reperfusion of the Ischemic Kidney. *Mol. Med.*, 14: 502–516.
20. **Lomeli N.; Di K.; Czerniawski J., Guzowski J.F. and Bota D.A. (2017):** Cisplatin-induced mitochondrial dysfunction is associated with impaired cognitive function in rats. *Free Radic Biol Med.*, 102: 274–286.

21. **Marullo, R.; Werner E.; Degtyareva N.; Moore B.; Altavilla G.; Ramalingam S. and Doetsch P. (2013):** Cisplatin Induces a Mitochondrial-ROS Response That Contributes to Cytotoxicity Depending on Mitochondrial Redox Status and Bioenergetic Function. *PLoS ONE* 8(11): e81162.
22. **Mishima, K.; Baba, A.; Matsuo, M.; Itoh, Y.; Oishi, R. (2006):** Protective effect of cyclic AMP against cisplatin-induced nephrotoxicity. *Free Radic. Biol. Med.*, 40(9): 1564-1577.
23. **Ozkurt, M.; Uzuner, K.; Erkasap, N.; Kus, G.; Ozyurt, R.; Uysal, O.; Akyazi, I. And Kutlay, O. (2018):** Erythropoietin Protects the Kidney by Regulating the Effect of TNF- α in L-NAME Induced Hypertensive Rats. *Kidney Blood Press. Res.*, 43: 807-819.
24. **Pabla, N. and Dong, Z. (2008):** Cisplatin nephrotoxicity: Mechanisms and renoprotective strategies. *Kidney Int.*, 73, 994–1007.
25. **Perše, M. and Haler, C.T. (2018):** pages Cisplatin-Induced Rodent Model of Kidney Injury: Characteristics and Challenges. *Hindawi Bio.Med. Research International*, Volume 2018, Article ID 1462802, 29 pages.
26. **Rashed, L.A.; Hashem, R.M. and Soliman, H.M. (2011):** Oxytocin inhibits NADPH oxidase and P38 MAPK in cisplatin-induced nephrotoxicity, *Biomed. Pharmacother.*, 65(7): 474–480.
27. **Rjiba-Touati, K.; Boussema, I.A.; Belarbia, A.; Achour, A. and Bacha, H. (2011):** Protective Effect of Recombinant Human Erythropoietin against Cisplatin- Induced Oxidative Stress and Nephrotoxicity in Rat Kidney *International Journal of Toxicology*, 30(5): 510-517.
28. **Rivkin, M.; Simerzin, A.; Zorde-Khvaleyevsky, E.; Chai, C.; Yuval, J.B.; Rosenberg, N.; Harari-Steinfeld, R.; Schneider, R.; Amir, G.; Condiotti, R.; Heikenwalder, M.; Weber, A.; Schramm, C.; Wege, H.; Kluwe, J.; Galun, E. And Giladi, H. (2016):** Inflammation-Induced Expression and Secretion of MicroRNA 122 Leads to Reduced Blood Levels of Kidney-Derived Erythropoietin and Anemia. *Gastroenterology*, 151: 999-1010.
29. **Sabine, L.; Hultström, M.; Rosenberger, C. and Iversen, B. (2011):** Afferent arteriopathy and glomerular collapse but not segmental sclerosis induce tubular atrophy in old spontaneously hypertensive rats. *Virchows Arch*, 459(1): 99–108.
30. **Sánchez-González, P.D.; López-Hernandez. F.J.; López-Novoa, J.M. and Morales, A.I. (2011):** An integrative view of the pathophysiological events leading to cisplatin nephrotoxicity. *Crit. Review Toxicol.*, 41: 803-821.
31. **Schrier, R.W. (2007):** Diseases of the kidney and urinary Tract, 8th Edition, volume II, pp: 930-962.
32. **Sonoda, H.; Oshikawa-Hori, S. and Ikeda, M. (2019):** An Early Decrease in Release of Aquaporin-2 in Urinary Extracellular Vesicles After Cisplatin Treatment in Rats. *Cells*, 8(2), 139
33. **Souma, T., Suzuki, N., & Yamamoto, M. (2015):** Renal erythropoietin-producing cells in health and disease. *Frontiers in physiology*, 6(167), doi:10.3389/fphys.2015.00167
34. **Vickers, A.E.M.; Rose, K.; Fisher, R.; Saulnier, M.; Sahota, P. and Bentley, P. (2004):** “Kidney slices of human and rat to characterize cisplatin-induced injury on cellular pathways and morphology”. *Toxicologic Pathology*, 32(5): 577–590.
35. **Volarevic V.; Djokovic B.; Jankovic M.; Harrell R.; Fellabaum C.; Djonov V. and Arsenijevic N. (2019):** Molecular mechanisms of cisplatin-induced nephrotoxicity: a balance on the knife edge between renoprotection and tumor toxicity. *Journal of Biomedical Science*, 26(25): <https://doi.org/10.1186/s12929-019-0518-9>
36. **Wenger R.H. and Hoogewijs D. (2010):** Regulated oxygen sensing by protein hydroxylation in renal erythropoietin producing cells. *Am. J. Physiol, Renal Physiol.*, 298: 1287-1296.
37. **Widmaier E.P., Raff H. and Strang K.T. (2014):** *Vander's Human Physiology; the Mechanics of Body Function*, 14th Edition, Chapter 14: The Kidneys and Regulation of Water and Inorganic Ions, 484-525
38. **Winning F., Fleck R.A. and Glover L. (2016):** Preparation of Renal Tissue: Tips & Tricks for Viewing on the Transmission Electron Microscope Using a Mirror. *Imaging & Microscopy*
39. **Zhang B.; Ramesh G.; Norbury C.C. and Reeves W.B. (2007):** “Cisplatin-induced nephrotoxicity is mediated by tumor necrosis factor-alpha produced by renal parenchymal cells”. *Kidney International*, 72(1): 37–44.